COMMUN. MATH. SCI.
Vol. 15, No. 7, pp. 1843–1866

FRONT MIGRATION FOR THE DISLOCATION STRAIN IN SINGLE CRYSTALS*

NICOLAS VAN GOETHEM†

Abstract. A single crystal is considered, i.e., a smooth elastic body $\Omega \subset \mathbb{R}^3$ containing a high density of point-defects and dislocations. In particular, we consider prismatic dislocation loops which result as the primary manifestation of irradiated or highly-deformed crystals. We consider linearized elasticity and identify the macroscopic dislocation-induced strain and its trace, directly related to the presence of dislocations, as the basic model variables. Further, we rely on a previously-introduced tensor version of a Cahn–Hilliard system in the context of incompatible linearized elasticity and consider the point-defects collapse into prismatic loops, yielding some well-formed microstructure. By means of a formal asymptotic analysis, we determine the front dynamics and obtain as a result a tensor version of Mullins–Sekerka dynamics. The associated gradient-flow formalism is also investigated.

Keywords. dislocations; linear elasticity; incompatibility; Cahn–Hilliard system; evolution law; Second principle.

AMS subject classifications. 35J48; 35J50; 55J30; 35G31; 35K52; 35Q74.

1. Introduction

1.1. Foreword. Focussing on the mesoscopic scale, dislocations are seen as loops of all sizes or lines with endpoints on the body boundary. They appear either by applying high enough external forces, or by a size and temperature-dependent collapse of 3d aggregates of point defects (namely *point defect clusters* in the case of point defects in the form of *interstitials*, or the so-called *voids* in the case of *vacancies*, see [36]). Specifically, this phenomenon takes place at those material points where the density of point defects has become unstable (i.e., has reached a threshold), and hence dissolve and collapse to form stable structure such as two-dimensional dislocation clusters (i.e., families of dislocation loops of various sizes), by minimizing a certain (Gibbs) free energy (also related to the temperature and temperature gradient). Details on this phenomenon can be found in [18, 38, 40, 44]. According to [40] the other type of stable structure that could result from instability of 3d clusters, called B-defects, do exhibit relatively weak strain fields within the crystal. Hence we focus on A-defects such as dislocation clusters and interstitial-type dislocation loops whose associated strain field is of significant magnitude. These loops happen to form microstructures and patterns such as polygonization and dislocation walls. Such dislocation-assisted phase separation processes are the motivation of this work, where a macroscopic model is sought complying with basic thermodynamics principles. One severe issue when considering the mesoscale is that loops of several scales of magnitudes coexist in real crystals, that is, infinitesimal loops together with loops of the size of the crystal diameter. Therefore, our choice is to work at a macroscopic scale on a tensor field called the dislocation-induced strain, directly related to the stress tensor by the linear elastic law, and to the dislocation density tensor by the incompatibility operator. Alternative approaches such

*Received: July 14, 2016; accepted (in revised form): April 28, 2017. Communicated by John Lowengrub.
The author was supported by the FCT Starting Grant " Mathematical theory of dislocations: geometry, analysis, and modelling" (IF/00734/2013).

†Universidade de Lisboa, Faculdade de Ciências, Departamento de Matemática, CMAF+CIO, Alameda da Universidade, C6, 1749-016 Lisboa, Portugal (vangoeth@fc.ul.pt).http://webpages.fc.ul.pt/ nvgoethem

as atomistic simulations are very promising but out of reach for large samples in terms of computational cost [1]. We refer to [21] for consistent thermodynamics models at the macroscopic scale.

1.2. Prismatic loops of interstitial type. An important process where dislocations and point defect strongly interact is the irradiation of materials with particles that create atomic displacements which can induce significant microstructural alteration [17,51], such as radiation damage in crystals that contributes to the phenomenon of embrittlement [16]. Particle or laser irradiation causes the production of structural disorder with generation of a large amount of point defects. These point defects can organize into defects of higher dimension and stimulate the occurrence of non-equilibrium phenomena (see [13]). For instance, interstitial loops arrise in solids bombarded by high-energy radiation because this environnement produces sufficient quantities of self-interstitials. This mechanism (usually taking place at a uniform temperature of several hundred degrees) permits the nucleation of prismatic dislocation loops followed by their growth in directions controlled by the climb forces[1]. The interstitial loop consists of a disk-shaped layer of atoms (i.e., a plate-like or platelet structure), which is more stable than the same number of atoms dispersed in the lattice as self-interstitials. In general there also exist vacancy loops [20], but since they are intrinsically unstable at all temperatures, rather than forming platelet-loops, vacancy condensation would result in macroscopic voids (see [22]). Eventually, the accumulation of point defects into a prismatic dislocation loop makes the point defects disappear: in the case of vacancies in a plane, the adjacent planes collapse to form a perfect crystal, while in the case of interstitials these introduce an additional plane which is also defect free in the interior (see Figure 1.1). Moreover, they can grow or shrink only by the absorption of further defects, and are free to move conservatively only along the edges of the prism defined by the continuation of their perimeter along the crystallographic direction of their Burgers' vector. Further, at nucleation, they have pure edge character, but in some circumstances can tilt with respect to the prism axis, and acquire a screw component (see Figure 1.1). In general, the prismatic loops arrise after quenching, irradiation, or after plastic deformation, and their density being often very high, they can influence considerably the mechanical as well as some other physical properties of crystalline materials. It is important to note [25] that their stress field decreases more quickly with distance than that of straight individual dislocations, which leads to a much weaker mutual elastic interaction and to the possibility of formation of a very high local density of these defects and therefore of microstructure (see next Section). Typical diameters of these loops are a few hundred A° and their maximum density is 10^{15} to 10^{16} loops/cm^3. This mechanism of precipitation of point defect in prismatic loops was originally proposed by Nabarro in 1947 [30] (i.e., in the case of vacancies) . Note that hexagonal or square loops are often observed experimentally, as related to the polygonization mechanism. First experimental evidences of the presence of prismatic loops where achieved in aluminium in 1958 as reported in [20].

1.3. Microstructure formation and Mullins–Sekerka front dynamics. Prismatic loops can also migrate (either vacancy-mediated or resulting from self-climb [42]) away from their glide cylinder [15]. Moreover, some of these loops are highly mobile along their Burgers vector directions, while others have much higher migration barrier creating stationary sinks for point defects. The interaction of all these mecha-

[1]The driving force for it being either the dislocation line tension [25] acting on the parts of the prismatic loop not lying in the glide plane, or the super- or under-saturation of point defect.

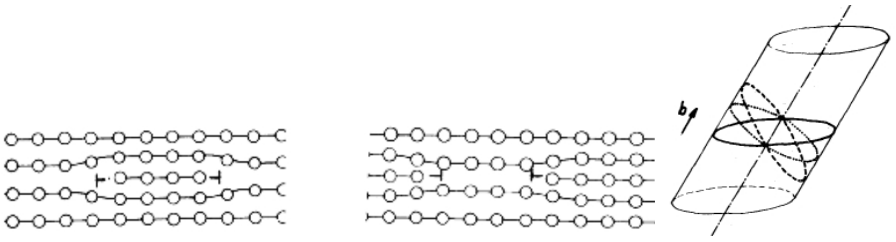

FIG. 1.1. *Prismatic loop: formation of an interstitial (left) and vacancy (middle) loop; and motion inside its glide cylinder (right: taken from [25]).*

nisms is very complex and yet not fully understood, but it is known that they result in loop coalescence [42], and give rise to a wide range of important plasticity mechanisms including network coarsening (see, e.g., [6]), creep, swelling and hardening. Moreover, mechanical or thermal polygonization [39], and recrystallization phenomena are also observed in bent and annealed crystals (the first work on this subject is by R. W. Cahn[2] [10], see also [14]). A sample of the variety of microstructure that is found in single crystals is shown in Figure 1.2. It is observed that (i) point defect clusters form plate-like structures (see black structures in Figure 1.2 in copper (above left) and nickel (middle)); (ii) by coalescing and collapsing they may form interstitial loops (stacking fault loops as in Figure 1.2 below left); (iii) they may coarsen in precise substructures as in Figure 1.2 (rightmost) where the interstitial clusters have collapsed to form cells with vanishing point-defect density in their interior, whereas the black regions show a complex coexistence and interaction of loops and clusters.

1.4. Scope of the work. In the present work, no specific mechanism will be investigated (i.e., whether irradiation or mechanical power is used to create defect substructures). We consider platelet aggregates of interstitial point defects and prismatic loops such as the black structures observed in Figure 1.2 (middle and rightmost). These point defects and loops interact, possibly coalescing, annihilating, migrating: they form some microstructure, which separates the crystal in two regions, one with high and the other with vanishing point defect density (cf. the black and white regions in the above images). So, thickening the interface, an unstable state is observed where prismatic loops and point defect aggregates coexist, whereas the perfect interface would exactly separate the crystal in two regions with are in thermodynamic equilibrium, the first with and the second without point defects. In the foregoing discussion, our goal is to model the dynamics of these complex defect structures as a point-defect and dislocation-mediated phase separation mechanism at the macroscale.

Coarsening dynamics are gradient flow dynamics, meaning that the evolution of an out-of-equilibrium system towards relaxation follows the steepest descent in an energy landscape. The descent in an energy landscape corresponds to reduction of the interface, and the pattern formed by the two phases "coarsens" [33]. Moreover, phase separation in alloys is known to obey the scalar Cahn–Hilliard equation (see [32] for a review, see also [37]).

In this work we rely on a tensor Cahn–Hilliard system derived in a previous contribution [47] and, interested in coarsening mechanisms, we are indeed concerned with

[2]Not to be confused with the other famous metallurgist J. W. Cahn whom the Cahn–Hilliard equation is due.

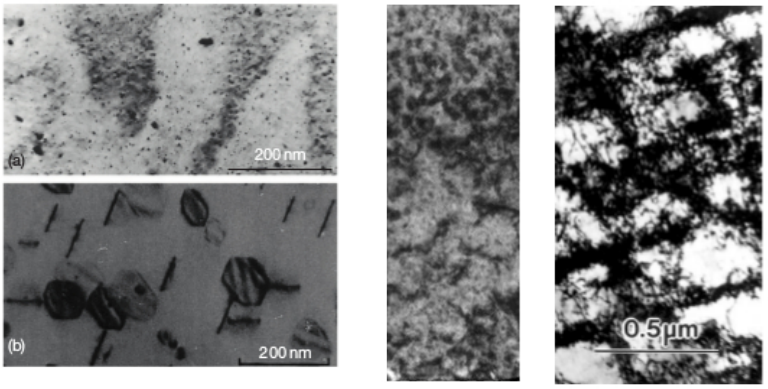

FIG. 1.2. *Observed microstructure: Microstructure produced in Copper single crystal following irradiation near 200 °C with fission neutrons (above; interstitial clusters of maximal size of 30 nm) and 1 MeV electron (below: moderate density of large faulted interstitial loops). Self-interstitial cluster patterning in Nickel (middle, from [23], height of the sample is 1 μm). Recrystalization in Copper: one observes low-dislocation-density inside the cells (left: modified from [31]).*

its sharp-interface counterpart, known as the Mullins–Sekerka problem (originally associated with solidification [29], see also [26] for crystal growth). The Mullins–Sekerka problem preserve volume and decrease surface energy and it is a non-local problem in that the motion of the surfaces cannot be ascertained without taking in consideration the behavior within the entire domain containing the interfaces [37]. We consider the macrosopic scale, where the fields are assumed smooth enough, that is the elastic strain is at least square integrable. Let us consider the stress tensor σ and the linear strain $\epsilon = \mathbb{A}^{-1}\sigma$, where $\mathbb{A}$ is the assumed constant and isothermal elasticity tensor, i.e., $\mathbb{A} = 2\mu\mathbb{I}_4 + \lambda\mathbb{I}_2 \otimes \mathbb{I}_2$, where $\mathbb{I}_4$ and $\mathbb{I}_2$ are the fourth- and second-rank identity tensors, respectively[3], with μ, λ the Lamé coefficients. The stress is symmetric by conservation of kinetic momentum, therefrom the strain is also a symmetric tensor, and thus writes by Beltrami decomposition [28] as $\epsilon = \nabla^S u + \epsilon^0$, where $\nabla^S u := \frac{1}{2}(\nabla u + \nabla^t u)$ with u, the generalized displacement vector and ϵ^0, the incompatibility strain, i.e., the part of the elastic strain which is incompatible. The macroscopic Kröner's relation (introduced in [24] and proved at the mesosopic scale in [48], see also [49]) reads $\mathrm{inc}\epsilon := \mathrm{Curl}\ \mathrm{Curl}^t\ \epsilon = \mathrm{inc}\epsilon^0 = \mathrm{Curl}\ \kappa$, where κ is the contortion tensor, as defined from the dislocation density Λ by the relation $\kappa = \Lambda - \frac{\mathbb{I}_2}{2}\mathrm{tr}\Lambda$, and with symbols Curl and Curl^t denoting the curl and transpose curl operator, here acting on tensors. In general Λ^t is divergence-free to account for the fact that dislocations are closed loops, as opposed to κ^t. Because of Kröner's relation, tensor ϵ^0 is called the dislocation-induced strain. The starting point of this work is to consider this latter tensor is the main model variable.

1.5. Linearized elasticity with dislocations and defect-induced density. The strain energy density in small-strain elasticity and for an isotropic material reads $W_e(\epsilon) = \frac{1}{2}\mathbb{A}\epsilon \cdot \epsilon$, where ϵ is the linearized elastic strain tensor. The stress tensor is classically defined as $\sigma := \delta_\epsilon W_e = \mathbb{A}\epsilon$. Furthermore, by the symmetry property of ϵ, Beltrami decomposition holds, viz., $\epsilon = \nabla^S u + \mathrm{inc}F$, with the dislocation-induced strain,

[3] Componentwise, $(\mathbb{I}_4)_{ijkl} = \frac{1}{2}(\delta_{ik}\delta_{jl} + \delta_{il}\delta_{jk})$, and $(\mathbb{I}_2)_{ij} = \delta_{ij}$.

$\epsilon^0 = \mathrm{inc}F$. The potential energy is defined as $\mathcal{W}(\epsilon) = \int_\Omega (W_e(\epsilon) - f\cdot u - \mathbb{G}\cdot F)\,dx$, where $\mathbb{G}$ is an externally applied load related to dislocations and incompatibility not further discussed here. Note that in the absence of dislocations, i.e., as soon as $F=0$, one has by minimization the standard equilibrium equation, $-\mathrm{div}(\mathbb{A}\epsilon) = -\mathrm{div}\left(\mathbb{A}\nabla^S u\right) = f$, with f the body force and u the displacement field. Now, in the general case where dislocations are present, the minimization problem writes as $\min_\epsilon \mathcal{W}(\epsilon) = \min \mathcal{W}(\epsilon)$ among all (u,F) such that $\epsilon = \nabla^S u + \mathrm{inc}F$, whose associated Euler–Lagrange equations read in the strong forms $-\mathrm{div}\sigma = f$ and $\mathrm{inc}\sigma = \mathbb{G}$, that show clearly as a generalization of the standard elasticity system in the presence of dislocations. Therefore, one must solve the coupled problem with unknowns u and F:

$$\begin{cases} -\mathrm{div}\left(\mathbb{A}\nabla^S u\right) &= f + \mathrm{div}\left(\lambda \mathrm{tr}\epsilon^0 \mathbb{I}_2\right), \\ \mathrm{inc}\left(\mathbb{A}\,\mathrm{inc}F\right) &= \mathbb{G} - \mathrm{inc}\left(\lambda \mathrm{div}u \mathbb{I}_2\right). \end{cases} \tag{1.1}$$

As based on the preliminary works [4,28,45], the latter two being specifically dedicated to the analysis of the incompatibility operator, some results and developments can be found on this generalized elasticity system, see [46,47]. In particular, the work [47] is devoted to develop and justify a dynamical law for the dislocation-induced strain ϵ^0.

Defect-induced density. Observing the problem (1.1), it is remarked that the mechanical Equation (1.1)a (in a classical divergence form) is found with a non-standard term on its right-hand side, namely a force proportional to the gradient of $\mathrm{tr}\epsilon^0$. On the other hand, the (dual) incompatibility Equation (1.1)b shows $\mathrm{div}u$ on its RHS, i.e., the variation of matter density due to mechanical efforts. It is now observed that $\mathrm{tr}\epsilon^0$ is exactly a variation of matter density due to incompatibility, i.e., to the presence of dislocations and point defects. Specifically, it may be understood as a density of point defects, since it will increase or decrease the local mass density, if interticials or vacancies, respectively, are present. This scalar $e := \mathrm{tr}\epsilon^0$ will play a crucial role in our model.

1.6. Describtion of the model. We assume that $\mathrm{tr}\epsilon^0$ models the density of point defects and that for a certain threshold e_*, the density reaches a critical value such that the point-defect aggregates collapse to form dislocation loops. We consider the previously formed and smooth time-evolving dislocation front Σ that separates Ω in two subdomains Ω^+ and Ω^-, with Ω^- enclosed by Σ. It is assumed that Σ is approximated by a transition layer of thickness ε and denoted by the volume Σ_ε. Point defects assume values close to the critical points 0 and e_* in $\Omega^+ \setminus \Sigma_\varepsilon$ and $\Omega^- \setminus \Sigma_\varepsilon$, respectively, whereas their density is unstable in the thick interface Σ_ε, with values between 0 and e_*, that is, Σ_ε is an unstable region of the crystal containing 3d interstitial clusters of various sizes together with prismatic loops which result from the collapse of platelet point defect aggregates. Let us emphasize that in the region where $\mathrm{tr}\epsilon^0$ is close to the critical value e_* the density of dislocations might be zero somewhere, in particular inside the point defect plate-like structures which are ready to collapse to form prismatic dislocation loops at their boundary. Note that after collapse, the point defect density inside these platelets is also vanishing since one recovers the bulk structure. Further, one should keep in mind that the limit $\varepsilon \to 0$ is an idealization where the crystal would be separated in a bulk region and a prismatic loop region resulting from the collapse of point-defects, see Figure 1.3. Indeed, physics (see Figure 1.2) rather corresponds with a finite value of ε).

1.7. Overview of the results. For dimensional homogeneity, we scale the chemical potential associated to this process (i.e., the functional derivative of the asso-

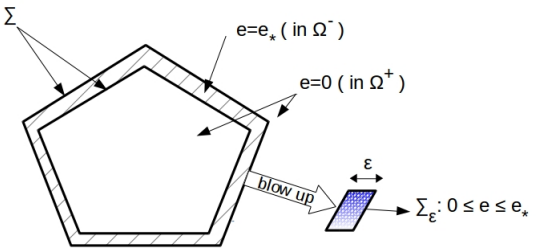

FIG. 1.3. *Schematic dislocation-induced microstructure* 3d *cell: low-point-defect density (i.e.,* $e=0$*) in* Ω^+ *critical (i.e.,* $e=e_*$*) inside* Ω^-*. The thickened interface* Σ_ε *is filled with dislocation dipoles, prismatic loops and point defect clusters in an unstable thermodynamic configuration.*

ciated Ginsburg–Landau energy $\mathscr{E}_\varepsilon$, see Section 3.5 for precise definitions) and get an ε-dependent potential μ_ε with a term in $\mathscr{O}(\varepsilon)$, another in $\mathscr{O}(1)$, and the last in $\mathscr{O}(\varepsilon^{-1})$. For this reason it is postulated that μ_ε satisfies the Ansatz $\mu_\varepsilon = \varepsilon^{-1}\mu_0 + \mu_1 + \varepsilon\mu_2 + \cdots$ for some zeroth-to-second order potentials to be determined by asymptotic analysis. Accordingly, the dislocation-induced strain is taken of the form $\epsilon^0_\varepsilon = \epsilon^0_0 + \varepsilon\epsilon^0_1 + \varepsilon^2\epsilon^0_2 + \cdots$. We consider the formal passage to the limit $\varepsilon \to 0$ and our main question is to found the asymptotic front velocity $V = \partial_t \Sigma$. Our main results are the following:

(1) We determine that μ_0 is constant in each phase. Moreover, $\mu_1(x,t)$ satisifies $\mathrm{inc}\mu_1 = 0$ in each phase, is fixed on Σ to a value depending on the front mean curvature $\mathrm{H}(x,t)$ and lower order fields.

(2) The tangential traces of μ_1 on Σ yield the value the front normal velocity.

(3) The front dynamics can be summarized by the following non-local Mullins–Sekerka law:

$$\begin{cases} \Delta \mathrm{tr}\mu_1 &= M(\mathrm{tr}\epsilon^0_1) & \text{in } \Omega^+ \cup \Omega^- \\ \mathrm{tr}\mu_1 &= m(\tilde{\epsilon}^0_0, \tilde{\epsilon}^0_1, \mathrm{tr}\epsilon^0_1) & \text{on } \Sigma \\ \partial_t \Sigma &= -e_*^{-1}\left(s(\mathrm{tr}\tilde{\epsilon}^0_0) + \{\partial_N \mathrm{tr}_{\mathrm{T}}\mu_1\}_\Sigma\right) & \\ \Sigma(0) &= \Sigma_0 & \end{cases},$$

where the $\sim$ symbol indicated a field blow-up close to Σ, and with an appropriate condition on the external boundary depending on the dislocation density and the strain. Let us emphasize a special, nonclassical feature of the system nonlocality, namely $\mathrm{H} = 0 \not\Rightarrow m = 0$, which allows us to treat interfaces with $\mathrm{H} = 0$, i.e., associated to polygonal structures (polygonization, see Figure 4.1).

2. Preliminary results: the mathematical setting

2.1. Notations, conventions, and functional spaces. Let $\Omega \subseteq \mathbb{R}^3$ be a simply-connected domain with smooth boundary. Let $E \in \mathbb{S}^3$ and $T \in \mathbb{M}^3$, where $\mathbb{M}^3$ denotes the space of square 3-matrices, and $\mathbb{S}^3$ of symmetric 3-matrices. superscript t stands for the transpose of a tensor and subscript S for the symmetric part of a tensor. The divergence curl and curl transpose of a tensor E are defined componentwise as $(\mathrm{div}E)_i := \partial_j E_{ij}$, $(\mathrm{Curl}\ E)_{ij} := \epsilon_{jkl}\partial_k E_{il}$, and $(\mathrm{Curl}^t\ E)_{ij} = \epsilon_{ikl}\partial_k E_{jl}$ respectively, where symbol ∂_i stands for the ith partial derivative, either in the strong or in classical distribution sense. Now, the incompatibility of a tensor E is the symmetric tensor defined componentwise as

follows[4]:

$$(\mathrm{inc}E)_{ij} := (\mathrm{Curl}\ \mathrm{Curl}^t\ E)_{ij} = \epsilon_{ikm}\epsilon_{jln}\partial_k\partial_l E_{mn}. \tag{2.1}$$

It holds $(E\times N)_{ij} = -(N\times E)_{ij} = -\epsilon_{jkm}N_k E_{im}$. Define

$$\begin{aligned}\mathcal{H}(\Omega) &:= \{E\in H^2(\Omega,\mathbb{S}^3) : \mathrm{div}E = 0 \text{ in } \Omega\},\\ \mathcal{H}_0(\Omega) &:= \{E\in\mathcal{H}(\Omega) :\ E = \mathrm{Curl}^t\ E\times N = 0 \text{ on } \partial\Omega\}.\end{aligned} \tag{2.2}$$

These spaces are naturally endowed with the Hilbertian structure of $H^2(\Omega,\mathbb{S}^3)$. Further more, symbol $\langle\cdot\rangle$ means in general "duality product", whereas the scalar product is written as $(\cdot)$, possibly with a subscript indicating the associated functional space. We enote by U^S the symmetric part of a tensor U.

2.2. The curvinormal frame. We denote by $N_{\partial\Omega}$ the outward unit normal to $\partial\Omega$, and by b the signed distance to $\partial\Omega$, i.e., $b(x) = \begin{cases}\mathrm{dist}(x,\partial\Omega) \text{ if } x\notin\Omega,\\ -\mathrm{dist}(x,\partial\Omega) \text{ if } x\in\Omega.\end{cases}$. We recall the following result.

THEOREM 2.1 ([12], Chap. 5, Thms 3.1 and 4.3). *There exists an open neighborhood W of $\partial\Omega$ such that (i) b is smooth in W, (ii) every $x\in W$ admits a unique projection $p_{\partial\Omega}(x)$ onto $\partial\Omega$, (iii) this projection satisfies $p_{\partial\Omega}(x) = x - \frac{1}{2}\nabla b^2(x),\quad \forall x\in W$, (iv) it holds $\nabla b(x) = N_{\partial\Omega}(p_{\partial\Omega}(x)),\quad \forall x\in W$.*

We define the extended unit normal by $N(x) := \nabla b(x) = N_{\partial\Omega}(p_{\partial\Omega}(x))$, $\forall x\in W$. For all $x\in\partial\Omega$, the system $(\tau^A_{\partial\Omega}(x),\tau^B_{\partial\Omega}(x),N_{\partial\Omega}(x))$ is an orthonormal basis of $\mathbb{R}^3$, where $\tau^R_{\partial\Omega}$ stand for the Rth tangent vector to $\partial\Omega$. In this basis, $DN(x)$ takes the form

$$DN(x) = \begin{pmatrix}\kappa^A_{\partial\Omega}(x) & 0 & 0\\ 0 & \kappa^B_{\partial\Omega}(x) & 0\\ 0 & 0 & 0\end{pmatrix},\qquad \forall x\in\partial\Omega,$$

where $\kappa^A_{\partial\Omega}$ and $\kappa^B_{\partial\Omega}$ are smooth scalar fields (the surface curvatures) defined on $\partial\Omega$. If $R\in\{A,B\}$, we denote by R^* the complementary index of R, that is, $R^* = B$ if $R = A$ and $R^* = A$ if $R = B$. Let us suitably extend the tangent vectors to W. It holds

THEOREM 2.2 (Amstutz–Van Goethem [4]). *The following holds in W:*

$$\begin{aligned}&\partial_N\tau^R = 0, \partial_R N = \kappa^R\tau^R, \partial_R\tau^R = -\kappa^R N - \gamma^{R^*}\tau^{R^*}, \partial_{R^*}\tau^R = \gamma^R\tau^{R^*},\\ &\mathrm{div}\ N = \mathrm{tr}DN = \Delta b = 2\mathrm{H},\end{aligned} \tag{2.3}$$

where scalar H *stands for the mean curvature.*

Let us consider the local orthonormal basis (τ^A,τ^B,N) in $\bar\Omega$. For a general symmetric tensor E, one has in this basis:

$$E = \begin{pmatrix}E_{AA} & E_{AB} & E_{AN}\\ E_{BA} & E_{BB} & E_{BN}\\ E_{NA} & E_{NB} & E_{NN}\end{pmatrix},\quad \mathcal{T}_0(E) := (E\times N)^t\times N = \begin{pmatrix}E_{BB} & -E_{AB} & 0\\ -E_{AB} & E_{AA} & 0\\ 0 & 0 & 0\end{pmatrix}. \tag{2.4}$$

Moreover, we define $\mathcal{T}_R(E) := \sum_{R=A,B}(E\times\tau^R)^t\times\tau^R$ with

$$(E\times\tau^A)^t\times\tau^A = \begin{pmatrix}0 & 0 & 0\\ 0 & E_{NN} & -E_{BN}\\ 0 & -E_{BN} & E_{BB}\end{pmatrix}, (E\times\tau^B)^t\times\tau^B = \begin{pmatrix}E_{NN} & 0 & -E_{AN}\\ 0 & 0 & 0\\ -E_{AN} & 0 & E_{AA}\end{pmatrix}. \tag{2.5}$$

[4]The last expression stemming from the symmetry of the incompatibility operator.

Having defined the tangential operator $\mathcal{T}_0$, one defines the tangential trace operator as

$$\mathrm{tr}_{\mathrm{T}}E := \mathrm{tr}\mathcal{T}_0(E). \tag{2.6}$$

Let us emphasize that the term tangential is used to mean orthogonal to the normal direction, the latter not being limited to the domain boundary, since the normal has been suitably extended, together with the tangent vectors, in the interior of the domain.

2.3. Functional results with the incompatibility operator.

THEOREM 2.3 (Beltrami decomposition [28]). *Let $p\in(1,+\infty)$ be a real number and let $E\in L^p(\Omega,\mathbb{S}^3)$ be a symmetric tensor. Then, there exist a vector field $u\in W^{1,p}(\Omega,\mathbb{R}^3)$ and a tensor $F\in L^p(\Omega,\mathbb{S}^3)$ with* Curl $F\in L^p(\Omega,\mathbb{S}^3)$, $\mathrm{inc}F\in L^p(\Omega,\mathbb{S}^3)$, $\mathrm{div}F=0$ *in Ω and $FN=0$ on $\partial\Omega$, where N stands for the unit normal to $\partial\Omega$, satisfying*

$$E=\nabla^S u+\mathrm{inc}\ F.$$

Moreover u can be taken with vanishing trace on $\partial\Omega$, and such a pair (u,F) is unique.

The following result is a Green formula.

LEMMA 2.1 (Amstutz–Van Goethem, 2016 [4]). *Suppose that $E\in\mathcal{C}^2(\overline{\Omega},\mathbb{S}^3)$ and $\eta\in H^2(\Omega,\mathbb{S}^3)$. Then*

$$\int_\Omega E\cdot\mathrm{inc}\eta dx=\int_\Omega \mathrm{inc}E\cdot\eta dx+\int_{\partial\Omega}\mathcal{T}_1(E)\cdot\eta\ dS(x)+\int_{\partial\Omega}\mathcal{T}_0(E)\cdot\partial_N\eta dS(x), \tag{2.7}$$

with the trace operators defined as

$$\mathcal{T}_0(E):=(E\times N)^t\times N, \tag{2.8}$$

$$\mathcal{T}_1(E):=-\sum_R\kappa^R(E\times\tau^R)^t\times\tau^R+((-\partial_N+2\mathrm{H})E\times N)^t\times N-2\left(\sum_R(\partial_R E\times N)^t\times\tau^R\right)^S. \tag{2.9}$$

As a consequence of technical results found in [4], one has

$$\begin{aligned}-\mathcal{T}_1(E)+2\mathrm{H}\mathcal{T}_0(E)&=\sum_R\kappa^R(E\times\tau^R)^t\times\tau^R+\mathcal{T}_0(\partial_N E)+2\left(\sum_R(\partial_R E\times N)^t\times\tau^R\right)^S,\\&=\sum_R\kappa^R(E\times\tau^R)^t\times\tau^R-\mathcal{T}_0(\partial_N E)-2\left(\mathrm{Curl}^t\ E\times N\right)^S.\end{aligned} \tag{2.10}$$

THEOREM 2.4 (Coercivity: Amstutz–Van Goethem, 2016 [4]). *Let Ω be a bounded and connected domain with $\mathcal{C}^1$-boundary and let the nowhere flat subset $\Gamma_0\subset\partial\Omega$ with $\mathcal{H}^2(\Gamma_0)>0$. There exists a constant $C>0$ s.t. for each $E\in\mathcal{H}_0(\Omega)$, $\|E\|_{H^2(\Omega)}\leq C\|\mathrm{inc}E\|_{L^2(\Omega)}$.*

3. The model

We consider a single crystal with a high density of point defects and dislocations. Prismatic loops are simply one type of point-defect aggregate. They will form from point defect clusters when their energy of formation is lower than other competing structures (e.g. 3d aggregates). The thermodynamic mechanism consists in free energy minimiziation, i.e., the lowest free energy configuration wins. Typically loops (of interstitial types) become more favorable as the size of the point defect cluster grows.

Then, if the overall kinetics is favorable, the cluster will transition to loop structures. In this work, we consider a crystal with 3d aggregates of interstital point defects and interstitial loops resulting from their collapse. While the former are unstables above a threshold, the latter are the stable structures. Another stable structure is of course the absence of interstitials, i.e., their self-annihilation, or dilution.

3.1. Dissipation, gradient flows: origin of the model. Gradient flows are evolutionary systems driven by an energy, in the sense that the energy decreases along solutions. This decrease takes place "as fast as possible" by choosing a dissipation mechanism, which is typically given by the choice of a norm, i.e., of a functional structure. Therefore, from a modelling point of view the two choices of the driving energy $\mathscr{E}$, and the dissipation mechanism completely determine the system. For instance, it is well known that the diffusion equation $\partial_t u = \Delta u$ is a gradient flow, that is, writes as $\partial_t u = -\mathrm{grad}_H \mathscr{E}(u)$, according to several possible choices of disspation mechanisms H (here symbol grad_H stands for the gradient flow associated to the functional $\mathscr{E}(u)$ with the norm of H), i.e., chosen norms, see [35] for details. Having said that, we rather agree with L. Tartar [43] that such a gradient flow minimization should not be considered as a physical principle, since as soon as time is present in the model, conservation law must prevail. Therefore, it might happen that energy conservation and minimization principles coincide, but the latter should rather be seen as a mathematical "vue de l'esprit".

In this work, we focus on a linear elastic body which is incompatible due to the presence of defects, and refer to [47] for details. We first introduce a specific Helmholtz free energy as $\Psi = W_{\mathrm{e}}(\epsilon) + \beta\kappa^S \cdot \kappa^S + \frac{1}{2}\mathbb{M}\mathrm{Curl}\,\kappa \cdot \mathrm{Curl}\,\kappa + \psi_{\mathrm{dislo}}(\epsilon^0)$ (the curl of a tensor is defined in Section 2.1 and $\mathbb{M}$ is a material-dependent fourth-rank tensor), to emphasize the role of the internal variables such as the dislocation density κ (via a postulated quadratic law) and the dislocation-induced strain ϵ^0 (through a nonlinear potential ψ_{dislo}). Note that the quadratic energy contributions involving the dislocation density can be found in other models [8], whereas the last contribution is a newly-introduced term. Let $\mathcal{D}$ be the global mechanical dissipation associated with Ψ, i.e., whose specific density is the difference between the power produced by internal forces upon deformation[5], $\sigma \cdot \dot{\epsilon}$, and the available, "free" energy $\dot{\Psi}$. Let Φ be the dissipated energy, i.e., $\mathcal{D} = -\frac{d}{dt}\Phi$. We define the incompatibility energy as part of the dissipated energy,

$$\mathscr{E}(\epsilon^0) := \int_\Omega \left(\frac{1}{2}\mathbb{M}\mathrm{inc}\epsilon^0 \cdot \mathrm{inc}\epsilon^0 + \mathscr{H}(\epsilon^0) \right) dx \tag{3.1}$$

(where we have used Kröner's relation $\mathrm{inc}\epsilon^0 = \mathrm{Curl}\,\kappa$ [24, 49]) and also introduce the "chemical potential" as $\mu(\epsilon^0) := -\left(\mathbb{M}\mathrm{inc}\epsilon^0 + \mathscr{G}(\epsilon^0)\right)$ for some divergence-free tensor potential $\mathscr{G}$ related to some energy density $\mathscr{H}$, both to be defined below. Note that $\mu(\epsilon^0)$ is not divergence-free for a general $\mathbb{M}$.

It has been derived in [47] that the non-negativeness of $\mathcal{D}$ resulting from the second Law of Thermodynamics implies that

$$0 \le \mathcal{D}_{\mathrm{incomp}} = \langle \mathrm{inc}\mu, \partial_t \epsilon^0 \rangle = -\langle \mathrm{grad}^{\mathcal{H}}_{\mathcal{H}_0^{-1}} \mathscr{E}(\epsilon^0), \partial_t \epsilon^0 \rangle = -\partial_t \mathscr{E}(\epsilon^0).$$

Therefore, the model can be written either in the form of a tensor-valued evolution transport-reaction-diffusion PDE of the following Cahn–Hilliard type:

$$\alpha \partial_t \epsilon^0 = \mathrm{inc}\mu = -\mathrm{inc}\left(\mathbb{M}\mathrm{inc}\epsilon^0 + \mathscr{G}(\epsilon^0)\right), \quad \alpha > 0, \tag{3.2}$$

[5]Note however that in [47] $\sigma \cdot \nabla^S \dot{u}$ was considered, leading to some supplementary terms.

whose trace reads as the scalar diffusion equation $\alpha\partial_t \mathrm{tr}\epsilon^0 = \Delta \mathrm{tr}\mu$ if μ is divergence-free (and thus, exactly corresponds to the classical scalar Cahn–Hilliard equation for the scalar variable $\mathrm{tr}\epsilon^0$, see [32] for a review), or as the gradient flow

$$\alpha\partial_t \epsilon^0 = -\mathrm{grad}^{\mathcal{H}}_{\mathcal{H}_0^{-1}} \mathscr{E}(\epsilon^0),$$

for an appropriate functional structure, whose determination is one of the purposes of this paper. For gradient flow dynamics in the present context we also refer to [7] (in particular to the chapter by R. Pego). Though the system evolution may be understood from a mathematical viewpoint as a gradient-driven free energy minimization, we know that the physical process need not be minimization driven, since as shown in [47], it is a consequence of the second law of thermodynamics.

3.2. Scalar variable and nonlinear potential. The model variable being the dislocation-induced strain tensor ϵ^0, let us introduce the scalar

$$e := \mathrm{tr}\epsilon^0, \tag{3.3}$$

which is a measure for the amount of point defects of interstitial type (and hence is nonnegative). In fact, the trace of the strain is directly related to the change of specific mass. Here, it is postulated that the trace of the dislocation-induced strain is related to the "non-mechanical" variations of density, i.e., to the amount of point defect which will increase (in the case of interstitials) or decrease (in the case of vacancies) the density of the solid, see [36]. Specifically, we assume that for a certain "threshold" value e_* the point-defect aggregates collapse to form prismatic dislocation loops, and hence the region $\{e \sim e_*\}$ is called the dislocated subset of Ω, though strictly speaking it is a critical region for the dislocation strain: it consists of a region where dislocation loops coexist with unstables 3d aggregates and isolated point defects, and subjected to an overall kinetics, which is not discussed in this work. The physical phenomena and processes associated with point defects (such a creation, annihilation, migration, diffusion, etc.) are represented by a nonlinear potential ϕ which assumes two local minima, the first being chosen as the thermodynamic equilibrium corresponding to the absence of point defects, and the other being the stability threshold (inducing the collapse of point defects, see Figure 1.3, see also leftmost image in Figure 1.2).

We postulate that this kinetics is represented by a two-well potential $\phi(e) = \frac{1}{2}((e - e^{\mathrm{eq}})\ (e - e_*))^2 + \gamma(e - e^{\mathrm{eq}}) + \phi_{\mathrm{eq}}$ with $\gamma, \phi_{\mathrm{eq}} \geq 0$. Setting $e^{\mathrm{eq}} = \phi_{\mathrm{eq}} = 0$, we assume that the equilibrium value corresponds to the absence of point defects[6]. Moreover, as far as minimization is concerned ϕ is insensitive to affine functions, since it would simply change the value of the minimum by an additive constant, leaving the local minimizers as unchanged. Therefore, we let the local minima of ϕ take distinct values at $e = e^{\mathrm{eq}} = 0$ and at $e = e_*$, that is, we consider the following nonlinear potential:

$$\phi(e) = \frac{1}{2}\left(e(e - e_*)\right)^2 + \gamma e. \tag{3.4}$$

In other words, $e^{\mathrm{eq}} = 0$ and e_* are the two local minima of ϕ such that at equilibrium of point defects, $\phi(e^{\mathrm{eq}}) = \phi(0) = 0$, whereas at the critical value e_* for the nucleation of dislocation loops, $\phi^* := \phi(e_*) = \gamma e_*$. We remark that $\lim_{e\to\infty} \phi''(e) = \infty$, thence ϕ'' is bounded from below, which is a required property for the existence result in [47]. Moreover

[6] It is usually considered that $e_* > e^{\mathrm{eq}} > 0$, but we remark that this simply amount to a translation of the energy function, which is impactless on the forthcomming theoretical developments.

$\phi'(0)=\phi'(e_*)=\gamma$, $\phi''(0)=\phi''(e_*)=e_*^2$ and $\phi'''(0)=-6e_*, \phi'''(e_*)=6e_*$. Furthermore, we assume that in the considered region there are no net creation or annihilation of point defects (though there exists recombinations of course), thence the total amount of point defects is prescribed, namely, $\int_\Omega e(x)dx=p>0$, where $0<p\leq e_*|\Omega|$.

REMARK 3.1. Since loops are more ordered (i.e., create less entropy) than other configurations, higher temperature will favor aggregates and the transition will take place at larger cluster sizes. This means that e_*, e^{eq}, p depend on the temperature T and that e_* increases with T. There is not a clear temperature for this transition, rather a temperature/size dependence, which is not further discussed here.

3.3. Model equations. Let $\mathbb{L}\in\mathbb{S}^3$ and $\mathbb{G}=\text{inc}\mathbb{L}$. As discussed in [47], let $\mathscr{G}=\mathcal{G}-\mathbb{L}$ in equation (3.2) and set

$$\mu(\epsilon^0):=-\left(\mathbb{M}\text{inc}\epsilon^0+\mathcal{G}(\epsilon^0)-\mathbb{L}\right), \quad \text{with} \quad \mathcal{G}(\epsilon^0):=\beta\epsilon^0-\frac{1}{3}\phi'(e)\mathbb{I}_2. \tag{3.5}$$

In this work we will consider the boundary-value problem (as derived and discussed in [47])

$$\begin{cases} \alpha\partial_t\epsilon^0-\text{inc}\mu(\epsilon^0)=0 & \text{in } \Omega\times[0,T] \\ (\epsilon^0)_{\text{T}}=(\partial_N\epsilon^0)_{\text{T}}=(\epsilon^0)_{NN}=0 & \text{on } \partial\Omega\times[0,T] \\ (\text{Curl}^t\ \epsilon^0)\times N=0 & \text{on } \partial\Omega\times[0,T] \\ \kappa^{R^*}(\mathbb{M}\text{inc}\epsilon^0)_{RN}+\partial_R(\mathbb{M}\text{inc}\epsilon^0)_{R^*R^*}-\partial_{R^*}(\mathbb{M}\text{inc}\epsilon^0)_{RR^*}=0 & \text{on } \partial\Omega\times[0,T] \end{cases}, \tag{3.6}$$

with $R=A,B$, where subscript $_{\text{T}}$ stands for the square submatrix with the tangential components. Moreover, the model parameters are the scalar $\alpha>0$ and the fourth-rank symmetric positive definite tensor $\mathbb{M}$ (assumed with the same symmetry as the elasticity tensor).

Well-posedness. Well-posedness of system (3.6) relies on the coercivity of the form $\langle\mathbb{M}\text{inc}E,\text{inc}E\rangle$, itself relying on the relation $\|E\|_{H^2(\Omega,\mathbb{S}^3)}\leq C\|\text{inc}E\|^2_{L^2(\Omega,\mathbb{S}^3)}$ for some $C>0$. The latter stems from the three following properties: (i) Poincaré inequality with the assumption $E_T=0$ (or alternatively $EN=0$) on $\partial\Omega$; (ii) the fact the the gradient of a divergence-free field F might be bounded by its curl provided that $F\times N=0$ (or alternatively that $FN=0$) on $\partial\Omega$; and finally from the relation $(\partial_l E)\times N=0$ (or alternatively $(\partial_l E)N=0$) on $\partial\Omega$ for every $l=1,2,3$ (see, e.g. [4, 9]). The first two conditions are satisfied by the boundary conditions of system (3.6) (take $E=\epsilon^0$ and $F=\text{Curl}^t\ \epsilon^0$). As for the the third, it is a direct consequence of Lemma 3.1 in [4], since $(\partial_N E)_T=\text{Curl}^t\ E\times N=0$ implies that $\epsilon_{jqv}N_v\epsilon_{mln}\partial_l E_{nj}=0$ which multiplied by ϵ_{mpq} and by the symmetry of E yields $(\partial_l E)\times N=0$. Now, with the addition of low-order terms the coercivity might be lost for the associated elliptic system, but not for the evolution equation (3.6), by the classical change of variable trick $\tilde{E}=\exp(-\xi_0 t)E$ for some $\xi_0>0$ (see, e.g., [3]).

REMARK 3.2. If $EN=0$ holds on $\partial\Omega$ then the divergence-free property of E yields (See Eq. (2.16) in [4]) $\partial_N E_{NN}-\sum_R\kappa^R E_{RR}=0$, itself implying that $(\partial_l E)N=0$ on $\partial\Omega$ for every $l=1,2,3$ and hence the form is coercive. This property was used without proof in [47].

REMARK 3.3 (Generalized elasticity). Let $\mathbb{K}\in\mathbb{S}^3$ be a prescribed generalized force. In [5] we have established the system of generalized elasticity as (i) $\text{inc}(\mathbb{A}\epsilon+\ell\text{inc}\epsilon)=$

$\mathrm{inc}\mathbb{K}$ coupled with (ii) $-\mathrm{div}(\mathbb{A}\epsilon+\ell\,\mathrm{inc}\epsilon)=-\mathrm{div}\mathbb{K}$, with the total strain $\epsilon=\nabla^S u+\epsilon^0$ and $\mathbb{A}=2\mu\mathbb{I}_4+\lambda\mathbb{I}_2\otimes\mathbb{I}_2$ the tensor of elasticity. Eq. (ii) yields a functional dependence of $\mathrm{div}u=\mathrm{tr}\nabla^S u$ in terms of $e=\mathrm{tr}\epsilon^0$. Therefore equation (i) rewrites as $\mathrm{inc}(2\mu\epsilon^0+\ell\,\mathrm{inc}\epsilon^0+\psi(e)\mathbb{I}_2-\mathbb{K})=0$ for some function ψ, that is, is the stationnary system associated with equation (3.2) where the potential μ of definition (3.5) is taken with $\mathbb{M}=\ell\mathbb{I}_4, \beta=2\mu$, $\mathbb{K}=\mathbb{L}$ and $\psi=-\frac{1}{3}\phi'$.

3.4. Incompatibility energy: gradient flow and scaling. Recall the incompatibility energy (3.1), considered as a part of the dissipated energy, and define the potential $\mathscr{H}(\epsilon^0)=-(\mathbb{G},\epsilon^0)_{L^2}+\frac{\beta}{2}(\mathrm{Curl}^t\,\epsilon^0,\mathrm{Curl}\,\epsilon^0)_{L^2}-\frac{1}{3}\phi(e)$. Integration by parts yields $\langle \mathrm{inc}\mathcal{G}(\epsilon^0)-\mathbb{G},F\rangle=\lim\limits_{\eta\to 0}\dfrac{\mathscr{H}(\epsilon^0+\eta F)-\mathscr{H}(\epsilon^0)}{\eta}$, for every $F\in\mathcal{H}_0(\Omega)$ and where $\langle\cdot,\cdot\rangle$ denotes the pairing between $\mathcal{H}_0(\Omega)$ and $\mathcal{H}^{-1}:=(\mathcal{H}_0(\Omega))'$. Then, integration by parts, and the Green formula of Lemma 2.1, imply that that the Gâteau differential of $\mathscr{E}$ at $\epsilon^0\in\mathscr{C}_c^\infty(\Omega)$ in the direction $F\in\mathcal{H}_0(\Omega)$ reads

$$\langle \mathrm{grad}^{\mathcal{H}_0}_{L^2}\mathscr{E}(\epsilon^0),F\rangle:=\int_\Omega \mathrm{inc}\left(\mathbb{M}\mathrm{inc}\epsilon^0+\mathscr{G}(\epsilon^0)\right)\cdot F dx=\int_\Omega\left(\mathbb{M}\mathrm{inc}\epsilon^0+\mathscr{G}(\epsilon^0)\right)\cdot \mathrm{inc}F dx, \tag{3.7}$$

where we recall that $\mathscr{G}=\mathcal{G}-\mathbb{L}=\beta\epsilon^0-\frac{1}{3}\phi'(e)\mathbb{I}_2-\mathbb{L}$. Taking $\epsilon^0\in\mathcal{H}_0(\Omega)$, the distribution $\mathrm{inc}\left(\mathbb{M}\mathrm{inc}\epsilon^0+\mathscr{G}(\epsilon^0)\right)$ defines a linear map of $\mathcal{H}^{-1}$ precisely by the rightmost integral of equation (3.7).

Scaling. Tensor $\mathbb{M}$ has the dimensions of a force times a surface, scalar β of a force, while ϕ has the dimensions of a force divided by a surface. Thus, to keep these terms of the same order as characteristic surface areas increase or decrease, one should multiply $\mathbb{M}$ and divide ϕ by a parameter ε with the dimensions of an inverse surface, respectively. Set $\varepsilon:=\left(\frac{\text{characteristic thickness}}{\text{characteristic surface}}\right)^2$. The scaled energy functional reads

$$\mathscr{E}_\varepsilon(\epsilon^0):=\int_\Omega\left(\frac{1}{2}\varepsilon\mathbb{M}\mathrm{inc}\epsilon^0\cdot\mathrm{inc}\epsilon^0+\mathscr{H}_\varepsilon(\epsilon^0)\right)dx,$$

where $\mathscr{H}_\varepsilon(\epsilon^0)=-(\mathbb{G},\epsilon^0)_{L^2}+\frac{\beta}{2}(\mathrm{Curl}^t\,\epsilon^0,\mathrm{Curl}\,\epsilon^0)_{L^2}-\frac{1}{3}\varepsilon^{-1}\phi(\mathrm{tr}\epsilon^0)$.

For a general $\epsilon^0\in\mathcal{H}(\Omega)$, one defines by equation (3.7) the $\mathcal{H}^{-1}$-gradient as follows:

$$\langle \mathrm{grad}^{\mathcal{H}_0}_{\mathcal{H}^{-1}}\mathscr{E}_\varepsilon(\epsilon^0),F\rangle:=\int_\Omega\left(\varepsilon\mathbb{M}\mathrm{inc}\epsilon^0+\mathscr{G}_\varepsilon(\epsilon^0)\right)\cdot\mathrm{inc}F dx,\ \forall F\in\mathcal{H}_0(\Omega),$$

where $\mathscr{G}_\varepsilon(\epsilon^0):=\beta\epsilon^0-\frac{1}{3}\varepsilon^{-1}\phi'(e)\mathbb{I}_2-\mathbb{L}$. The linear and continuous map $\mathrm{grad}^{\mathcal{H}_0}_{\mathcal{H}^{-1}}\mathscr{E}_\varepsilon(\epsilon^0)$ is associated to a unique $G^0_\varepsilon\in\mathcal{H}_0$ such that $\mathrm{inc}\,\mathrm{inc}G^0_\varepsilon=\mathrm{inc}\left(\varepsilon\mathbb{M}\mathrm{inc}\epsilon^0+\mathscr{G}_\varepsilon(\epsilon^0)\right)$ and Riesz theorem yields $\langle \mathrm{grad}^{\mathcal{H}_0}_{\mathcal{H}^{-1}}\mathscr{E}_\varepsilon(\epsilon^0),F\rangle=\int_\Omega \mathrm{inc}G^0_\varepsilon\cdot\mathrm{inc}F dx$, the RHS being a scalar product on $\mathcal{H}_0$ by Theorem 2.4.

3.5. Dual functional spaces and gradient flow formalism. Set

$$\mathcal{H}_*(\Omega):=\{F\in\mathcal{H}(\Omega):FN=0\text{ on }\partial\Omega\},$$

and introduce the Hilbert space

$$\mathcal{H}_0^{-1}:=\left\{\mathcal{T}\in(\mathcal{H}(\Omega))':\exists\mathbb{T}\in\mathcal{H}_*(\Omega):\langle\mathcal{T},E\rangle=\int_\Omega\mathrm{inc}\mathbb{T}\cdot\mathrm{inc}E dx,\ \forall E\in\mathcal{H}(\Omega)\right\},$$

where $\langle\cdot,\cdot\rangle$ denotes the duality pairing between $\mathcal{H}(\Omega)$ and $(\mathcal{H}(\Omega))'$. Remark that such tensor $\mathbb{T}$ is unique since it is defined up to a symmetric gradient which must be

divergence-free, and hence vanishes by the boundary condition $\mathbb{T}N=0$. Let us call this unique tensor[7] $\mathbb{T}=\mathrm{inc}_*^{-2}\mathcal{T}$. We define the $\mathcal{H}_0^{-1}$-gradient as

$$\langle \mathrm{grad}^{\mathcal{H}}_{\mathcal{H}_0^{-1}}\mathscr{E}_\varepsilon(\epsilon^0),F\rangle := -\int_\Omega \mu_\varepsilon\cdot \mathrm{inc}F dx,\ \forall F\in\mathcal{H}(\Omega),$$

where we have introduced the "chemical potential" as the tensor

$$\mu_\varepsilon(\epsilon^0) := -\left(\varepsilon\mathbb{M}\mathrm{inc}\epsilon^0+\mathscr{G}_\varepsilon(\epsilon^0)\right) = -\mathrm{inc}\left(\mathrm{inc}_*^{-2}(\mathrm{grad}^{\mathcal{H}}_{\mathcal{H}_0^{-1}}\mathscr{E}_\varepsilon(\epsilon^0))\right)\in L^2(\Omega,\mathbb{S}^3).$$

The gradient $\mathrm{grad}^{\mathcal{H}}_{\mathcal{H}_0^{-1}}\mathscr{E}_\varepsilon(\epsilon^0)$ is the dual of μ_ε in the sense that $\mathrm{inc}\mu_\varepsilon=-\mathrm{grad}^{\mathcal{H}}_{\mathcal{H}_0^{-1}}\mathscr{E}_\varepsilon(\epsilon^0)=-\mathrm{inc}\left(\varepsilon\mathbb{M}\mathrm{inc}\epsilon^0+\mathscr{G}_\varepsilon(\epsilon^0)\right)$. Therefore, our model evolution equation (3.6)a rewrites as the following $\mathcal{H}_0^{-1}$-gradient flow:

$$\partial_t\epsilon^0 = -\frac{1}{\alpha}\mathrm{grad}^{\mathcal{H}}_{\mathcal{H}_0^{-1}}\mathscr{E}_\varepsilon := -\frac{1}{\alpha}\mathrm{inc}\left(\varepsilon\mathbb{M}\mathrm{inc}\epsilon^0+\mathscr{G}_\varepsilon(\epsilon^0)\right)=\frac{1}{\alpha}\mathrm{inc}\mu_\varepsilon, \tag{3.8}$$

where the ε-dependent solution of equation (3.8) will be denoted by ϵ^0_ε in the sequel. In particular, we see that the driving force for diffusion is the incompatibility of the dislocation potential. Indeed, it can be noted that taking the trace of equation (3.8) yields $\partial_t\mathrm{tr}\epsilon^0_\varepsilon=\frac{1}{\alpha}(\Delta\mathrm{tr}\mu_\varepsilon-\mathrm{div}\,\mathrm{div}\mu_\varepsilon)$. We remark that if $\mathbb{M}$ has the form $\mathbb{M}=2\tilde{\mu}\mathbb{I}_4+\tilde{\lambda}\mathbb{I}_2\otimes\mathbb{I}_2$, the highest-order term of the RHS reads $-\frac{2\varepsilon}{\alpha}(\tilde{\mu}+\tilde{\lambda})\Delta\mathrm{tr}\epsilon^0_\varepsilon$, yielding the classical scalar Cahn–Hilliard equation.

4. Asymptotic analysis

The analysis in the present section will be made in the spirit of R. Pego's work [34] for the classical scalar Cahn–Hilliard system. The analysis is formal but its main purpose here is to identify the equations and the jump conditions in our tensor-valued and incompatibility-based setting. The interested reader may find rigourous results about the classical Cahn–Hilliard system in, e.g., [2,11,27]. It is assumed that the time-evolving front Σ with unit normal N separates the domain in two subdomains Ω^+ and Ω^- (with Ω^- possibly disconnected), where $\partial\Omega=\partial\Omega^+$, i.e., Ω^- is enclosed by Σ. Moreover, it is assumed that Σ is approximated by a smooth thick interface a width of order $\varepsilon>0$, and therefore the associated transition layer is denoted by the volume Σ_ε (see Figure 1.3). Furthermore, we consider the dynamics second stage, i.e., we assume that the interface has been formed previously, is smooth at the initial time $t=0$, and that the point defects assume values close to the critical points 0 and e_* in $\Omega^+\setminus\Sigma_\varepsilon$ and $\Omega^-\setminus\Sigma_\varepsilon$, respectively. Therefore, we are concerned with the evolution of the dislocation strain ϵ^0, and the evolution of the interface. In particular, we seek the front (otherwise called, interface) velocity $V:=\partial_t\Sigma$. Setting

$$\mathscr{L}(\epsilon^0):=\beta\epsilon^0-\mathbb{L}, \tag{4.1}$$

equation (3.8) rewrites as (recall the definition $e:=\mathrm{tr}\epsilon^0$)

$$\alpha\partial_t\epsilon^0_\varepsilon=\mathrm{inc}\mu_\varepsilon,\quad \mu_\varepsilon:=-\varepsilon\mathbb{M}\mathrm{inc}\epsilon^0_\varepsilon-\mathscr{L}(\epsilon^0_\varepsilon)+\frac{1}{3}\varepsilon^{-1}\phi'(\mathrm{tr}\epsilon^0_\varepsilon)\mathbb{I}_2. \tag{4.2}$$

The initial value is prescribed, i.e., $\epsilon^0_\varepsilon(\cdot,0)=\epsilon^0_{00}$ and satisfies $\int_\Omega\mathrm{tr}\epsilon^0_{00}dx=p>0$. For simplicity we take $\alpha=1$.

[7] This notation arrise from the fact that for smooth tensors one has $\mathrm{incinc}\mathbb{T}=\mathcal{T}$ by taking E with compact support.

4.1. Far-from-the-front. Let us expand $\epsilon^0_\varepsilon, e_\varepsilon := \mathrm{tr}\epsilon^0_\varepsilon$ and μ_ε as powers of ε:

$$\begin{cases} \epsilon^0_\varepsilon &= \epsilon^0_0 + \varepsilon\epsilon^0_1 + \varepsilon^2\epsilon^0_2 + \cdots \\ e_\varepsilon &= e_0 + \varepsilon e_1 + \varepsilon^2 e_2 + \cdots \\ \mu_\varepsilon &= \varepsilon^{-1}\mu_0 + \mu_1 + \varepsilon\mu_2 + \cdots \end{cases}, \tag{4.3}$$

where $\epsilon^0_i, e_i := \mathrm{tr}\epsilon^0_i$ and μ_i are functions of x and t. Note that ϵ^0_i are divergence-free tensors. Moreover, the boundary trace $\epsilon^0_{|\partial\Omega} = \epsilon^0_{0|\partial\Omega}$ and hence $\epsilon^0_1 = \epsilon^0_2 = 0$ on $\partial\Omega$. By identification, definition (4.2) yields

$$\begin{cases} \mu_0 &= \frac{1}{3}\phi'(e_0)\mathbb{I}_2 \\ \mu_1 &= \frac{1}{3}\phi''(e_0)e_1\mathbb{I}_2 - \mathscr{L}(\epsilon^0_0) \\ \mu_2 &= \frac{1}{6}\phi'''(e_0)e_1^2\mathbb{I}_2 + \frac{1}{3}\phi''(e_0)e_2\mathbb{I}_2 - \mathbb{M}\mathrm{inc}\epsilon^0_0 - \beta\epsilon^0_1 \end{cases}. \tag{4.4}$$

Order-zero solution. Expanding equation (4.2) with the expressions (4.3), taking its trace, and considering the order -1 term yields $\Delta\phi'(e_0) = \phi'''(e_0)|\nabla e_0|^2 + \phi''(e_0)\Delta e_0 = 0$, whose case study (in function of the zeroes of ϕ'' and ϕ''' and the maximum principle) entails that e_0 is constant, i.e.,

$$e_0 = 0 \text{ in } \Omega^+, \quad e_0 = e_* \text{ in } \Omega^-. \tag{4.5}$$

From a physical viewpoint, the fact that $e_0 = e_*$ reflects the fact that the collapse of the point-defect platelet in prismatic loops will take place with the release of the residual strain e_*.

Then $\phi'(0) = \phi'(e_*) = \gamma$ yields

$$\mu_0 = \frac{\gamma}{3}\mathbb{I}_2, \quad \partial_N\mu_0 = 0 \text{ in } \Omega. \tag{4.6}$$

Recalling that $\phi''(0) = \phi''(e_*) = e_*^2$, we note that

$$\mathrm{tr}\mu_1 = e_*^2 e_1 - \beta e_0 + \mathrm{tr}\mathbb{L} \quad \text{and} \quad \mathrm{div}\mu_1 = \frac{1}{3}e_*^2\nabla e_1 + \mathrm{div}\mathbb{L} \quad \text{in} \quad \Omega^+\cup\Omega^-. \tag{4.7}$$

Time evolution, far from the front. The time-evolution in $\Omega\times[0,T]$ reads

$$\begin{cases} 0 &= \mathrm{inc}\mu_0 \\ \partial_t\epsilon^0_0 &= \mathrm{inc}\mu_1 \\ \partial_t\epsilon^0_1 &= \mathrm{inc}\mu_2 \end{cases}. \tag{4.8}$$

The constant value of e_0 in $\Omega^+\cup\Omega^-$, the relations $\mathbb{G} = \mathrm{inc}\mathbb{L}$ and $\phi''(e_0) = e_*^2$ imply that $0 = \partial_t e_0 = \mathrm{tr}\,\mathrm{inc}\mu_1 = \Delta\,\mathrm{tr}\mu_1 - \mathrm{div}\,\mathrm{div}\mu_1$, and hence by equation (4.7),

$$\begin{cases} -\eta\Delta e_1 &= \mathrm{tr}\mathbb{G} \text{ in } \Omega^+\cup\Omega^- \\ \partial_N e_1 &= 0 \quad \text{on} \quad \Sigma \\ e_1 &= 0 \quad \text{on} \quad \partial\Omega \end{cases}, \tag{4.9}$$

with $\eta := \frac{2}{3}e_*^2$. Thus, e_1 is determined as soon as Σ is known, which is the ultimate goal of this work.

Long-time behaviour. Let us define the slow time as $t^*=\varepsilon^{-1}t$. Then, following equation (3.8), far from the front one has $\alpha\partial_{t^*}\epsilon^0=\varepsilon \mathrm{inc}\mu_\varepsilon$, and equation (4.8) yields $\partial_{t^*}\epsilon^0_0=\mathrm{inc}\mu_0=0$, and hence ϵ^0_0 remains at its initial value $\epsilon^0_{00}:=\epsilon^0_0(\cdot,0)$, i.e.,

$$\epsilon^0_0(\cdot,t)=\epsilon^0_{00} \text{ in } \Omega \quad \text{and} \quad e_0=\begin{cases} 0 & \text{in } \Omega^+ \\ e_* & \text{in } \Omega^- \end{cases}. \tag{4.10}$$

Recapitulating, by virtue of expressions (4.4)-(4.10), one has in $\Omega\times[0,T]$,

$$\begin{cases} \mu_0 = \frac{\gamma}{3}\mathbb{I}_2 \\ \mu_1 = \frac{1}{3}\phi''(e_0)e_1\mathbb{I}_2-\mathscr{L}(\epsilon^0_{00})=\frac{1}{3}e_*^2e_1\mathbb{I}_2-\beta\epsilon^0_{00}+\mathbb{L} \\ \mu_2 = \frac{1}{6}\phi'''(e_0)e_1^2\mathbb{I}_2+\frac{1}{3}\phi''(e_0)e_2\mathbb{I}_2-\mathbb{M}\mathrm{inc}\epsilon^0_{00}-\beta\epsilon^0_1 \\ \quad = \begin{cases} -e_*e_1^2\mathbb{I}_2+\frac{1}{3}e_*^2e_2\mathbb{I}_2-\beta\epsilon^0_1 & \text{in } \Omega^+ \\ e_*e_1^2\mathbb{I}_2+\frac{1}{3}e_*^2e_2\mathbb{I}_2-\beta\epsilon^0_1 & \text{in } \Omega^- \end{cases} \end{cases}. \tag{4.11}$$

4.2. Close-to-the-front. Let $b(x,t)$ stand for a time-dependent signed distance function from Σ, as introduced in Section 2.2. In particular $b>0$ in Ω^+ and $b<0$ in Ω^-. Furthermore, $\partial_t b(x,t)$ represents the velocity of the front for $x\in\Sigma$ (while $b(x,t)=0$ if $x\in\Sigma$). Define a stretched distance function $z:=\varepsilon^{-1}b(x,t)$. Let us expand ϵ^0 and μ_ε close to the interface, as powers of ε as follows:

$$\begin{cases} \epsilon^0_\varepsilon = \tilde{\epsilon}^0_0+\varepsilon\tilde{\epsilon}^0_1+\varepsilon^2\tilde{\epsilon}^0_2+\cdots \\ e_\varepsilon = \tilde{e}_0+\varepsilon\tilde{e}_1+\varepsilon^2\tilde{e}_2+\cdots \\ \mu_\varepsilon = \varepsilon^{-1}\tilde{\mu}_0+\tilde{\mu}_1+\varepsilon\tilde{\mu}_2+\cdots \end{cases}, \tag{4.12}$$

where $\tilde{\epsilon}^0_i,\tilde{e}_i$ and $\tilde{\mu}_i$ are now functions of x and t and of z. Introduce the following notations for a generic tensor E:

$$E=\bar{E}(x,t):=\tilde{E}(z,x,t), \quad z=\hat{z}(x;\varepsilon)=\varepsilon^{-1}b(x,t), \tag{4.13}$$

i.e., $\varepsilon^{-1}b$ is a streched normal distance. Moreover, one defines the jump across the interface as

$$[\![E(z)]\!]_\Sigma:=E(+\infty)-E(-\infty).$$

Thus, $\bar{\epsilon}^0_i(x,t):=\tilde{\epsilon}^0_i(z,x,t)=\tilde{\epsilon}^0_i(\varepsilon^{-1}b(x,t),x,t)$ and $\bar{\mu}_i(x,t):=\tilde{\mu}_i(\varepsilon^{-1}b(x,t),x,t)$. By equation (4.10), the matching conditions for the zeroth-order term reads[8]

$$\tilde{\epsilon}^0_0(z,x,t)\to\epsilon^0_0(x,t) \text{ as } z\to\pm\infty \quad \text{and} \quad \tilde{e}_0(z,x,t)\to\begin{cases} 0 & \text{as } z\to+\infty \\ e_* & \text{as } z\to-\infty \end{cases}. \tag{4.14}$$

Recalling that the extended normal, defined as $N:=\nabla b$ (i.e., pointing inwards Ω^+) is independent of the normal coordinate z, one has $\nabla\bar{E}(x,t)=\varepsilon^{-1}N\partial_z\tilde{E}(z,x,t)+\nabla_x\tilde{E}(z,x,t)$, and hence $\mathrm{Curl}\,\bar{E}(x,t)=\varepsilon^{-1}N\times\partial_z\tilde{E}(z,x,t)+\mathrm{Curl}_x\tilde{E}(z,x,t)$ and

$$\mathrm{div}\bar{E}(x,t)=\varepsilon^{-1}\partial_z\Big(\tilde{E}(z,x,t)N\Big)+\mathrm{div}_x\tilde{E}(z,x,t). \tag{4.15}$$

[8] In a suitable norm, say $\mathcal{C}^2$ for convenience.

Then, $\mathrm{inc}\bar{E}(x,t) = \mathrm{Curl}\,\left(\mathrm{Curl}^t\ E(x,t)\right) = \mathrm{inc}_x\tilde{E}(z,x,t) + \varepsilon^{-1}\mathcal{T}_2\left(\partial_z\tilde{E}(z,x,t)\right)$, where decomposing along the curvinormal frame and recalling the formulae of Theorem 2.2, one has (for a generic tensor $F = \bar{F}(x,t) := \tilde{F}(z,x,t)$,

$$\begin{aligned}(\mathcal{T}_2(F))_{mk} &:= \frac{1}{2}\epsilon_{mjn}\epsilon_{kpi}\left(\partial_p(N_jF_{in}) + \partial_j(N_pF_{in})\right)\\ &= \epsilon_{mjn}\epsilon_{kpi}\left(\sum_R \tau_j^R\tau_p^R\kappa^R F_{in} + \frac{1}{2}\left(N_j\partial_pF_{in} + N_p\partial_jF_{in}\right) + \varepsilon^{-1}N_jN_p\partial_z\tilde{F}_{in}\right).\end{aligned}$$

Moreover, by the definition of $\mathcal{T}_0$ (see definition (2.8)), from an index-wise computation one has $\mathcal{T}_2(F) = \varepsilon^{-1}\mathcal{T}_0(\partial_z\tilde{F}) + \mathcal{T}_3(F)$ where the operator $\mathcal{T}_3$ is defined as $\mathcal{T}_3(F) := \mathcal{T}_R(F) - \left((\mathrm{Curl}\ F)^t \times N\right)^S$, with $\mathcal{T}_R(F) = \sum_R \kappa^R(F\times\tau^R)^t\times\tau^R$. Setting

$$\mathcal{T}_4(F) := \frac{1}{2}\left(\mathcal{T}_0(\partial_N F) - \mathcal{T}_1(F)\right) \text{ and } \quad \mathcal{T}_{\mathrm{H}}(F) := \mathrm{H}\mathcal{T}_0(F) + \mathcal{T}_R(F),$$

and recalling equations (2.5), (2.8), (2.9) and (2.10), one obtains

$$\mathcal{T}_3(F) = \mathcal{T}_{\mathrm{H}}(F) + \mathcal{T}_4(F), \tag{4.16}$$

with H, the mean curvature. Taking $F = \partial_z\tilde{E}(z,x,t)$, the final expression for the incompatibility is found as

$$\mathrm{inc}\bar{E}(x,t) = \mathrm{inc}_x\tilde{E}(z,x,t) + \varepsilon^{-1}\mathcal{T}_3\left(\partial_z\tilde{E}(z,x,t)\right) + \varepsilon^{-2}\mathcal{T}_0\left(\partial_z^2\tilde{E}(z,x,t)\right). \tag{4.17}$$

Divergence-free condition. By virtue of equation (4.15), the divergence-free condition $\mathrm{div}\epsilon^0 = 0$ implies that

$$0 = \varepsilon^{-1}\partial_z\left(\tilde{\epsilon}_0^0N\right) + \left(\mathrm{div}_x\tilde{\epsilon}_0^0 + \partial_z\left(\tilde{\epsilon}_1^0N\right)\right) + \varepsilon\left(\mathrm{div}_x\tilde{\epsilon}_1^0 + \partial_z\left(\tilde{\epsilon}_2^0N\right)\right) + \varepsilon^2\,\mathrm{div}_x\tilde{\epsilon}_2^0,$$

therefrom $\tilde{\epsilon}_0^0N$ is independent of z, i.e.,

$$\tilde{\epsilon}_0^0(z,x,t)N(x,t) = \tilde{E}_0N(x,t) \tag{4.18}$$

for some $\tilde{E}_0$ depending on x and t only. In particular $\partial_z(\tilde{\epsilon}_0^0N\cdot N) = 0$, and hence

$$\partial_z(\mathrm{tr}\tilde{\epsilon}_0^0) = \partial_z(\mathrm{tr}_{\mathrm{T}}\ \tilde{\epsilon}_0^0), \tag{4.19}$$

where the tangential trace is given in definition (2.6). Moreover, the definition of μ_ε in (4.2) and equation (4.12) imply that the ε^{-2}-term must vanish, i.e.

$$\partial_z\tilde{\mu}_0N(z,x,t) = 0. \tag{4.20}$$

Dislocation potentials in the transition layer. By identification, the definition of μ_ε in (4.2) and equations (4.12) and (4.17) yield

$$\begin{cases}\tilde{\mu}_0 = \frac{1}{3}\phi'(\tilde{e}_0)\mathbb{I}_2 - \mathbb{M}\mathcal{T}_0\left(\partial_z^2\tilde{\epsilon}_0^0\right)\\ \tilde{\mu}_1 = \frac{1}{3}\phi''(\tilde{e}_0)\tilde{e}_1\mathbb{I}_2 - \mathscr{L}(\tilde{\epsilon}_0^0) - \mathbb{M}\mathcal{T}_3\left(\partial_z\tilde{\epsilon}_0^0\right) - \mathbb{M}\mathcal{T}_0\left(\partial_z^2\tilde{\epsilon}_1^0\right)\\ \tilde{\mu}_2 = \frac{1}{6}\phi'''(\tilde{e}_0)\tilde{e}_1^2\mathbb{I}_2 + \frac{1}{3}\phi''(\tilde{e}_0)\tilde{e}_2\mathbb{I}_2 - \mathbb{M}\mathrm{inc}_x\tilde{\epsilon}_0^0 - \beta\tilde{\epsilon}_1^0 - \mathbb{M}\mathcal{T}_3\left(\partial_z\tilde{\epsilon}_1^0\right) - \mathbb{M}\mathcal{T}_0\left(\partial_z^2\tilde{\epsilon}_2^0\right)\end{cases} \tag{4.21}$$

Differentiating equation (4.21)a in z and multiplying the result by $\tilde{e}_1$ yields $(\partial_z\tilde{\mu}_0)\tilde{e}_1 = \frac{1}{3}\phi''(\tilde{e}_0)\partial_z\tilde{e}_0\tilde{e}_1\mathbb{I}_2 - \mathbb{M}\mathcal{T}_0\left(\partial_z^3\tilde{\epsilon}_0^0\right)\tilde{e}_1$. Multiplying equation (4.21)b by $\partial_z\tilde{e}_0$ yields

$\left(\tilde{\mu}_1+\mathscr{L}(\tilde{\epsilon}_0^0)+\mathbb{M}\mathcal{T}_3\left(\partial_z\tilde{\epsilon}_0^0\right)\right)\partial_z\tilde{e}_0=\frac{1}{3}\phi''(\tilde{e}_0)\tilde{e}_1\partial_z\tilde{e}_0\mathbb{I}_2-\mathbb{M}\mathcal{T}_0\left(\partial_z^2\tilde{\epsilon}_1^0\right)\partial_z\tilde{e}_0$. Hence, substracting the two equalities, and anticipating the fact that $\partial_z\tilde{\mu}_0=0$ (see equation (4.31)), we deduce the following formula which we will use later:

$$\left(\tilde{\mu}_1+\mathscr{L}(\tilde{\epsilon}_0^0)+\mathbb{M}\mathcal{T}_3\left(\partial_z\tilde{\epsilon}_0^0\right)\right)\partial_z\tilde{e}_0=-\mathbb{M}\mathcal{T}_0\left(\partial_z^2\tilde{\epsilon}_1^0\partial_z\tilde{e}_0-\partial_z^3\tilde{\epsilon}_0^0\tilde{e}_1\right). \tag{4.22}$$

With a view to the final formulae let us compute the incompatibility in x of equation (4.21)a,

$$\mathrm{inc}_x\tilde{\mu}_0=\frac{1}{3}(\delta_{ij}\Delta-\partial_i\partial_j)\phi'(\tilde{e}_0)-\partial_z\left(\mathrm{inc}_x\mathbb{M}\mathcal{T}_0\left(\partial_z\tilde{\epsilon}_0^0\right)\right). \tag{4.23}$$

Asymptotic matching of the dislocation potentials. It is required that

$$(\varepsilon^{-1}\tilde{\mu}_0+\tilde{\mu}_1+\varepsilon\tilde{\mu}_2+\cdots)(z,x,t)\sim(\varepsilon^{-1}\mu_0+\mu_1+\varepsilon\mu_2+\cdots)(x+\varepsilon zN),t)$$

at a $\mathscr{O}(\varepsilon)$-distance from the interface. Recalling definition (4.13), one gets

$$\left\{\begin{array}{l}\tilde{\mu}_0(z,x,t)=\frac{\gamma}{3}\mathbb{I}_2\quad\text{as } z\to\pm\infty\\ \tilde{\mu}_1(z,x,t)=\mu_1(x,t)+z\partial_N\mu_0(x,t)+o(\varepsilon)\quad\text{as } z\to\pm\infty\\ \tilde{\mu}_2(z,x,t)=\mu_2^{\pm}(x,t)+\left(z\partial_N\mu_1+\frac{z^2}{2}\partial_N^2\mu_0\right)(x,t)+o(\varepsilon)\quad\text{as } z\to\pm\infty\end{array}\right. . \tag{4.24}$$

In particular, since μ_0 is constant, one has

$$\partial_z\tilde{\mu}_2=\partial_N\mu_1+o(\varepsilon)\quad\text{as } z\to\pm\infty, \tag{4.25}$$

thence a formula which will be used later:

$$\int_{-\infty}^{\infty}\partial_z^2\tilde{\mu}_2dz=\{\partial_N\mu_1\}_\Sigma+o(\varepsilon),\quad\text{as } z\to\pm\infty, \tag{4.26}$$

where we have introduced the following notation for the jump across Σ:

$$\{E(x,t)\}_\Sigma:=E\left(\mu_1(x^+,t)\right)-E\left(\mu_1(x^-,t)\right):=\lim_{\delta\to0}\left(E(x+\delta b,t)-E(x-\delta b,t)\right), \tag{4.27}$$

for a generic tensor E and recalling that $b(x,t)$ is the signed distance from the front.

Time evolution, close to the front. The front velocity is given by

$$\partial_t\Sigma:=V(x,t):=\partial_tb(x,t),\quad x\in\Sigma. \tag{4.28}$$

For a generic tensor $E=\bar{E}(x,t)=\tilde{E}(z,x,t)$, one has $\partial_t\bar{E}(x,t)=\partial_t\tilde{E}(z,x,t)+\varepsilon^{-1}V\partial_z\tilde{E}(z,x,t)$. Identification among equations (4.2), (4.16), and (4.17) yields the order ε^{-3},ε^{-2} and ε^{-1} as follows:

$$\left\{\begin{array}{rl}0&=\mathcal{T}_0\left(\partial_z^2\tilde{\mu}_0\right)\\ 0&=\mathcal{T}_3\left(\partial_z\tilde{\mu}_0\right)+\mathcal{T}_0\left(\partial_z^2\tilde{\mu}_1\right)\\ V\partial_z\tilde{\epsilon}_0^0&=\mathrm{inc}_x\tilde{\mu}_0+\mathcal{T}_3\left(\partial_z\tilde{\mu}_1\right)+\mathcal{T}_0\left(\partial_z^2\tilde{\mu}_2\right)\end{array}\right. . \tag{4.29}$$

Zeroth-order dislocation strain. Equation (4.29) a yields $0=\mathcal{T}_0\left(\partial_z^2\tilde{\mu}_0\right)$, i.e., recalling that $\mathcal{T}_0$ is a tangential operator, $\tilde{\mu}_0=A_0(x,t)z+\mathbb{B}_0(x,t)+C_0^N(z,x,t)=\mathbb{B}_0(x,t)+C_0^N(z,x,t)$, since $\tilde{\mu}_0$ is finite at $z\to\pm\infty$, and where C_0^N is a symmetric matrix such that its tangential submatrix vanishes, i.e., $\mathcal{T}_0(C_0^N)=0$. There is perfect phase separation away from the interface and hence equations (3.4), (4.14) and (4.21)a yield (recalling identities $\mathcal{T}_0(\mathbb{I}_2)=\mathbb{I}_2-N\otimes N$),

$$\mathcal{T}_0(\tilde{\mu}_0)=\mathbb{B}_{00}:=\mathcal{T}_0(\mathbb{B}_0)=\lim_{z\to+\infty}\mathcal{T}_0(\tilde{\mu}_0)=\lim_{z\to-\infty}\mathcal{T}_0(\tilde{\mu}_0)=\frac{1}{3}\gamma(\mathbb{I}_2-N\otimes N). \quad (4.30)$$

Moreover, equation (4.20) implies that $\mathbb{B}_0N+C_0^NN$ and hence also $C_0^N=C_0^NN$ is independent of z, and hence

$$\tilde{\mu}_0=\mathbb{B}_0(x,t). \quad (4.31)$$

Let us go back to equation (4.21)a, that is,

$$\partial_z^2\left(\mathcal{T}_0(\tilde{\epsilon}_0^0)\right)=\mathcal{T}_0\left(\mathbb{M}^{-1}\left(\frac{1}{3}\phi'(\tilde{e}_0)\mathbb{I}_2-\mathbb{B}_0\right)\right), \quad (4.32)$$

which is the tensor counterpart of the equation $y''=f(y)$, whose solution is obtained by considering the ODE $dy=\sqrt{2\int_{y_0}^y f(s)ds}dz$ for some well-chosen initial condition y_0. Let us denote the unique solution of equation (4.32) by

$$\mathbb{E}_0(z,x,t):=\mathcal{T}_0(\tilde{\epsilon}_0^0).$$

Hence, $\tilde{E}_0:=\tilde{\epsilon}_0^0=\mathbb{E}_0+\hat{C}_0^N$, where the last term might depend on z and satisfies $\mathcal{T}_0(\hat{C}_0^N)=0$. Yet by equation (4.18), $\tilde{E}_0N=(\mathbb{E}_0+\hat{C}_0^N)N=\hat{C}_0^NN$ is independent of z, that is, $\hat{C}_0^NN$ and thus $\hat{C}_0^N$ must be independent of z. Therefore,

$$\tilde{E}_0(z,x,t)=\mathbb{E}_0(z,x,t)+\hat{C}_0^N(x,t), \quad (4.33)$$

where the constant $\hat{C}_0^N=\bar{C}_0^N(x,t)$ is determined by matching the inner and outer solutions, viz., by virtue of equation (4.10) and (4.14),

$$\tilde{E}_0\to\epsilon_{00}^0 \text{ as } z\to\pm\infty \quad \text{and} \quad \tilde{e}_0:=\mathrm{tr}\tilde{E}_0\to\begin{cases}0 & \text{as } z\to+\infty\\ e_* & \text{as } z\to-\infty\end{cases}, \quad (4.34)$$

with

$$\partial_z\tilde{e}_0=\partial_x\tilde{e}_0=0 \text{ as } z\to\pm\infty. \quad (4.35)$$

Long-time behaviour. Let us define the slow time as $t^*=\varepsilon^{-1}t$ and the slow velocity as $V_{\mathrm{sl}}:=\partial_{t^*}b$, in such a way that $\partial_t\tilde{E}_0(x,t)=\varepsilon^{-1}\partial_{t^*}\tilde{E}_0(z,x,t)+\varepsilon^{-2}V_{\mathrm{sl}}\partial_z\tilde{E}_0(z,x,t)$ satisfies by equations (4.17), (4.31) and (4.33),

$$V_{\mathrm{sl}}\partial_z\mathbb{E}_0=\mathcal{T}_3\left(\partial_z\tilde{\mu}_0\right)+\mathcal{T}_0\left(\partial_z^2\tilde{\mu}_1\right)=\mathcal{T}_0\left(\partial_z^2\tilde{\mu}_1\right). \quad (4.36)$$

Taking the trace of equation (4.36), integrating from $-\infty$ to $+\infty$, and recalling definition (2.6), yields

$$V_{\mathrm{sl}}=[\![\mathrm{tr}_{\mathrm{T}}(\partial_z\tilde{\mu}_1)]\!]_\Sigma[\![\mathrm{tr}\mathbb{E}_0]\!]_\Sigma^{-1}, \quad (4.37)$$

where by expression (4.34),

$$[\![\tilde{e}_0]\!]_\Sigma=[\![\mathrm{tr}\mathbb{E}_0]\!]_\Sigma:=\mathrm{tr}E_0^+-\mathrm{tr}E_0^-=-e_*. \quad (4.38)$$

Equation (4.37) shows that to have an expression of the slow velocity, the next order must be determined in order to find an expression of $\tilde{\mu}_1$.

4.3. Close to the front: first-order terms. By equations (4.29)b and (4.31) it holds that $0=\mathcal{T}_0\left(\partial_z^2\tilde{\mu}_1\right)$ and hence the above reasoning can be repeated leading to

$$\tilde{\mu}_1=\mathbb{B}_1(x,t). \tag{4.39}$$

Therefore equation (4.21)b yields (recall that $\tilde{e}_0:=\mathrm{tr}\tilde{\epsilon}_0^0=\mathrm{tr}\tilde{E}_0$)

$$\partial_z^2\left(\mathcal{T}_0(\tilde{\epsilon}_1^0)\right)=\mathbb{M}^{-1}\left(\frac{1}{3}\phi''(\tilde{e}_0)\tilde{e}_1\mathbb{I}_2-\mathscr{L}(\tilde{E}_0)-\mathbb{M}\mathcal{T}_3(\partial_z\mathbb{E}_0)-\mathbb{B}_1\right), \tag{4.40}$$

which is of the same form as equation (4.32) and has a unique solution

$$\tilde{E}_1(z,x,t)=\mathbb{E}_1(z,x,t)+\tilde{C}_1^N(x,t). \tag{4.41}$$

Let us compute the integral of the RHS of equation (4.22) from $-\infty$ to $+\infty$. By expression (4.34), one has $\lim\limits_{z\to\pm\infty}\mathbb{E}_0'=\lim\limits_{z\to\pm\infty}\mathbb{E}_0''=0$, and hence integrating by parts yields

$$\int_{-\infty}^{+\infty}\left(\partial_z^3\mathbb{E}_0\,\mathrm{tr}\tilde{\epsilon}_1^0-\partial_z^2\tilde{\epsilon}_1^0\partial_z\tilde{e}_0\right)dz=\mathbb{V}_0:=-\int_{-\infty}^{+\infty}\left(\partial_z^2\mathbb{E}_0\partial_z\,\mathrm{tr}\mathbb{E}_1+\partial_z^2\mathbb{E}_1\partial_z\,\mathrm{tr}\mathbb{E}_0\right)dz,$$

which is a known value by virtue of equations (4.33) and (4.41). Note that for simplicity we have writen $\mathbb{E}_0'(z)$ to mean $\partial_z\mathbb{E}_0(z,x,t)$. Then, the tangential projection of equation (4.22) integrates as

$$\int_{-\infty}^{+\infty}\mathcal{T}_0\left(\tilde{\mu}_1+\mathscr{L}(\mathbb{E}_0)+\mathbb{M}\mathcal{T}_3(\partial_z\mathbb{E}_0)\right)\partial_z\tilde{e}_0dz=\mathbb{W}_0:=\mathcal{T}_0\left(\mathbb{M}\mathcal{T}_0(\mathbb{V}_0)\right), \tag{4.42}$$

which, recalling equation (4.39), implies that

$$\begin{aligned}&\int_{-\infty}^{+\infty}-\left(\mathcal{T}_0\left(\mathscr{L}(\mathbb{E}_0(z))\right)+\mathcal{T}_{0M3}\left(\mathbb{E}_0'(z)\right)\right)\partial_z\tilde{e}_0dz+\mathbb{W}_0\\&=\int_{-\infty}^{+\infty}\mathcal{T}_0(\mathbb{B}_1)\partial_z\tilde{e}_0dz=\mathcal{T}_0(\mathbb{B}_1)[\![\tilde{e}_0]\!]_\Sigma=-e_*\mathcal{T}_0(\mathbb{B}_1),\end{aligned} \tag{4.43}$$

by virtue of equation (4.38), and where we have defined the operator $\mathcal{T}_{0M3}:=\mathcal{T}_0\mathbb{M}\mathcal{T}_3$.

First-order potential on the interface. Equation (4.16) yields $\mathcal{T}_{0M3}(\mathbb{E}_0')=\mathcal{T}_0\left(\mathbb{M}\mathcal{T}_{\mathrm{H}}(\mathbb{E}_0')\right)+\mathcal{T}_0\left(\mathbb{M}\mathcal{T}_4(\mathbb{E}_0')\right)$, where we have defined the operators $\mathcal{T}_{0MH}:=\mathcal{T}_0\mathbb{M}\mathcal{T}_{\mathrm{H}}$ and $\mathcal{T}_{0M4}:=\mathcal{T}_0\mathbb{M}\mathcal{T}_4$. Hence the tangential part of the first-order potential $\tilde{\mu}_1$ writes by equations (4.39) and (4.43) as

$$\mathcal{T}_0(\tilde{\mu}_1)(x,t)=\mathcal{T}_0(\mathbb{B}_1)=\left(\mathbb{S}_{\mathrm{H}}(x,t)-\mathbb{Q}_0(x,t)\right)e_*^{-1},\quad x\in\Sigma, \tag{4.44}$$

where the following tensors (depending on (x,t) and independent of z) have been introduced:

$$\mathbb{S}_{\mathrm{H}}:=\int_{-\infty}^{+\infty}\mathcal{T}_0\left(\mathbb{M}\mathcal{T}_{\mathrm{H}}\left(\mathbb{E}_0'(z)\right)\right)\partial_z\tilde{e}_0dz, \tag{4.45}$$

$$\mathbb{Q}_0:=\left(\mathbb{W}_0-\int_{-\infty}^{+\infty}\left(\mathcal{T}_0\left(\mathbb{M}\mathcal{T}_4\left(\mathbb{E}_0'(z)\right)\right)+\mathcal{T}_0\left(\mathscr{L}(\mathbb{E}_0(z))\right)\right)\partial_z\tilde{e}_0dz\right). \tag{4.46}$$

Now, observe that equations (4.24)b and (4.6) yield $\tilde{\mu}_1(z,x,t)=\mu_1(x,t)+o(\varepsilon)$ as $z\to\pm\infty$. Hence considering expression (4.44) on the interface, i.e., as $\varepsilon\to0$, one has

$$\mathcal{T}_0(\mu_1)(x,t)=\left(\mathbb{S}_{\mathrm{H}}(x,t)-\mathbb{Q}_0(x,t)\right)e_*^{-1}. \tag{4.47}$$

4.4. Time-evolution of the dislocation front. The front Σ is assumed to be known at time t and its velocity $\partial_t\Sigma = V(x,t)$, where V is given in definition (4.28) and is obtained by integrating equation (4.29)c from $-\infty$ to $+\infty$ and letting $\varepsilon \to 0$. By virtue of equations (4.26) and (4.39), this yields

$$V[\![\mathbb{E}_0]\!]_\Sigma = \mathbb{P}_0 + \mathcal{T}_0(\{\partial_N \mu_1\}_\Sigma), \tag{4.48}$$

where $\mathbb{P}_0 := \int_{-\infty}^{+\infty} \mathrm{inc}_x \tilde{\mu}_0 dz$ can be written componentwise by equations (4.23), (4.3)b and (4.35) as

$$(\mathbb{P}_0)_{ij} = \int_{-\infty}^{+\infty} \frac{1}{3}(\delta_{ij}\Delta_x - \partial_i\partial_j)\phi'(\tilde{e}_0)dz. \tag{4.49}$$

Thus, we need to compute the jump of $\partial_N \mu_1$ in equation (4.48). To this aim, the asymptotic values of the far-field first-order potential μ_1 are required. By equations (4.8) and (4.10), one has

$$\partial_t \epsilon_0^0 = \partial_{t^*}\epsilon_0^0 = 0 = \mathrm{inc}\mu_1, \quad \text{in } \Omega^+ \cup \Omega^-, \tag{4.50}$$

with the value of the potential on the interface given by equation (4.47), namely,

$$\begin{cases} \mathcal{T}_0(\mu_1) = (\mathbb{S}_{\mathrm{H}} - \mathbb{Q}_0)e_*^{-1} & \text{on } \Sigma \\ \mathcal{T}_1(\mu_1) = 0 & \text{on } \Sigma \end{cases}.$$

Let $\mathbb{H}$ be a solution to

$$\begin{cases} \mathrm{inc}\,\mathrm{inc}\mathbb{H} &= 0 & \text{in } \Omega^+ \cup \Omega^- \\ \mathcal{T}_0(\mathrm{inc}\mathbb{H}) &= (\mathbb{S}_{\mathrm{H}} - \mathbb{Q}_0)e_*^{-1} & \text{on } \Sigma \\ \mathcal{T}_1(\mathrm{inc}\mathbb{H}) &= 0 & \text{on } \Sigma \\ \mathbb{H} = \mathcal{T}_0(\partial_N \mathbb{H}) &= 0 & \text{on } \partial\Omega \end{cases}. \tag{4.51}$$

Then $\mu_1 = \mathrm{inc}\mathbb{H} + \mathbb{C}$ for some compatible tensor $\mathbb{C}$. Further, it is easy to see that $\mathrm{inc}\mathbb{H}N = 0$ on $\partial\Omega$. Recalling equations (4.7) and (4.11)b, one has $\mathbb{C} = \nabla^S u$ with u solution of $\mathrm{div}\nabla^S u = \mathrm{div}\mu_1 = \frac{1}{3}e_*^2 \nabla e_1 + \mathrm{div}\mathbb{L}$ in $\Omega^+ \cup \Omega^-$, where e_1 is solution of equation (4.9) with $(\nabla^S u)N = 0$ on Σ and $(\nabla^S u)N = \mu_1 N = \mu N$ on $\partial\Omega$. Moreover, by Theorems 2.1 and 2.4, the variational problem associated to (4.51) is

$$\mathbb{H} = \underset{F \in \mathcal{H}_0(\Omega)}{\mathrm{argmin}} \left\{ \int_\Omega (\mathrm{inc}F)^2 dx + e_*^{-1} \int_\Sigma (\mathbb{S}_{\mathrm{H}} - \mathbb{Q}_0) \cdot \partial_N F dS(x) \right\}.$$

Further, the front velocity $V = \partial_t\Sigma$ depends on the jump at the interface of μ_1 and $\tilde{E}_0$ and reads by equation (4.48) and definition (4.27),

$$\begin{cases} [\![\mathbb{E}_0]\!]_\Sigma V &= \mathbb{P}_0 + \mathcal{T}_0(\{\partial_N \mu_1\}_\Sigma) \\ \Sigma(0) &= \Sigma_0 \end{cases}, \tag{4.52}$$

where $\mu_1 = \mathrm{inc}\mathbb{H} + \mathbb{C}$. Thus, $[\![\mathcal{T}_0(\mathbb{E}_0)]\!]_\Sigma V = \mathcal{T}_0(\mathbb{P}_0) + \{\partial_N \mathcal{T}_0(\mu_1)\}_\Sigma$. Taking the trace in the latter, and integrating equation (4.19), the front velocity reads

$$\begin{cases} \partial_t\Sigma &= [\![\mathrm{tr}_{\mathrm{T}}\mathbb{E}_0]\!]_\Sigma^{-1}(\mathrm{tr}_{\mathrm{T}}\mathbb{P}_0 + \{\partial_N \mathrm{tr}_{\mathrm{T}}\mu_1\}_\Sigma) = -e_*^{-1}(\mathrm{tr}_{\mathrm{T}}\mathbb{P}_0 + \{\partial_N \mathrm{tr}_{\mathrm{T}}\mu_1\}_\Sigma) \\ \Sigma(0) &= \Sigma_0 \end{cases}, \tag{4.53}$$

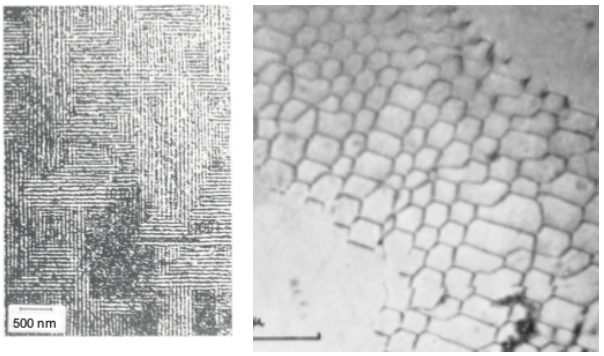

FIG. 4.1. *Observed microstructure with flat boundaries: defect cluster patterning into walls in SCS irradiated with protons (left: from [51]). Polygonization in magnesium-oxide single crystals (right: from [41])*

with $\mathrm{tr}_{\mathrm{T}}\mathbb{P}_0 := \mathrm{tr}\mathbb{P}_0 - \mathbb{P}_0 N\cdot N = \int_{-\infty}^{+\infty}\left(\frac{1}{3}\Delta_x\phi'(\tilde{e}_0) - \partial_N^2\phi'(\tilde{e}_0)\right)dz$.

Equations (4.51) and (4.53) constitute the global tensor-valued evolution system, analogous to the Mullins–Sekerka law obtained for the classical scalar Cahn–Hilliard equation [2, 11, 27]. Though, there exists a notable difference, namely that the right-hand side of equation (4.51) is given by a term proportional to the total curvature of the front, viz., $\mathbb{S}_{\mathrm{H}}$ (as in the Mullins–Sekerka law), plus a term, i.e., $-\mathbb{Q}_0$, that is independent of the curvature. Hence μ_1 will be nonzero even for flat interfaces (such as polygonal regions or flat walls, see Figure 4.1).

Now, let us deduce a scalar equation from the tensor-valued system (4.51): taking the traces of equations (4.51) a and b and recalling definition (2.6), one has by (4.4) and (4.9) $\mathrm{tr}(\mathrm{inc}\mu_1) = \Delta\mathrm{tr}\mu_1 - \mathrm{div}\,\mathrm{div}\mu_1 = 0$ and $\mathrm{tr}\mu_1 = \mathrm{tr}_{\mathrm{T}}\mu_1 + \mu_1 N\cdot N$. Thus,

$$\begin{cases} \Delta\mathrm{tr}\mu_1 = M \text{ in } \Omega^+\cup\Omega^- \\ \mathrm{tr}\mu_1 = m \qquad\quad \text{on } \Sigma \end{cases}, \tag{4.54}$$

where $M := \frac{1}{3}e_*^2\Delta e_1 + \mathrm{div}\,\mathrm{div}\mathbb{L}$ and $m := e_*^{-1}(\mathrm{tr}\mathbb{S}_{\mathrm{H}} - \mathrm{tr}\mathbb{Q}_0) + \frac{1}{3}e_*^2 e_1 + \mathbb{L}N\cdot N$, with e_1 the solution of equation (4.9) and recalling equation (4.11)b and the fact that $\mathrm{div}\epsilon_{00}^0 = 0$ in Ω implies that $\epsilon_{00}^0 N = 0$ on Σ. The scalar system (4.53) and (4.54) is similar to the classical Mullins–Sekerka law, the only difference being the terms on the right-hand side of equation (4.54)b independent of the front curvature. In fact, one has a system where the value of $\mathrm{tr}\mu_1$ is fixed on the interface, where in each phase one solves a Poisson problem. Moreover the interface has a velocity $\partial_t\Sigma$ that depends on the jump of the normal derivative of $\mathrm{tr}_{\mathrm{T}}\mu_1$ across the front, which we denote according to [27] as the restricted Laplacian to Σ, i.e., $\Delta_\Sigma(\mathrm{tr}\mu_1) := -\{\partial_N\mathrm{tr}\mu_1\}_\Sigma$. In particular, equation (4.54) may be rewritten as $\Delta\mathrm{tr}\mu_1 = M + \Delta_\Sigma m\delta_\Sigma$. Let us emphasize that because of the terms independent of the front curvature, the dynamics is more complex than gradient-flow area minimization, as in classical scalar Cahn–Hilliard [27], and in particular makes it possible to capture flat boundaries, which arrise in the actual crystals.

5. Concluding remark

This paper is a direct follow-up of the recent work [47] where a tensor version of Cahn–Hilliard system was derived in the context of incompatible linearized elasticity. Interpreting the trace of the incompatible strain as the density of point defects, in the

present paper we propose a model for point defects collapse into dislocation loops in single crystals as based on Cahn–Hilliard dynamics. Moreover, by means of asymptotic analysis, we determine the front dynamics. In particular we obtain a tensor version of Mullins–Sekerka law which allows for flat interfaces. As polygonization is an observed phenomena in single crystals with dislocations, this feature is of particular interest. The chosen asymptotic approach is required to determine the form of the equations, though rigourous results may also be derived in future works. The proposed approach is to the knowledge of the author the first macroscopic model to address the problem where the incompatibility strain is the main model variable. Other approaches exist at the macroscale as in [13, 16, 31, 42]. Further, alternative approaches are the atomistic simulations, which are very promising but still have a huge computational cost and thus are restricted to samples of limited size, see e.g., [19, 50]. It is yet an open question to determine to what extend this model is acceptable for engineers and practicioners.

REFERENCES

[1] R. Abu Al-Rub, *Continuum-based modeling of size effects in micro-and nanostructured materials*, in Handbook of Micromechanics and Nanomechanics, Pan Standford Publ., 2013.

[2] N.D. Alikakos, P.W. Bates, and X. Chen, *Convergence of the Cahn–Hilliard equation to the Hele-Shaw model*, Arch. Ration. Mech. Anal., 128(2):165–205, 1994.

[3] G. Allaire, *Numerical Analysis and Optimization. An Introduction to Mathematical Modelling and Numerical Simulation*, Translation from the French by Alan Craig., Oxford: Oxford University Press, 2007.

[4] S. Amstutz and N. Van Goethem, *Analysis of the incompatibility operator and application in intrinsic elasticity with dislocations*, SIAM J. Math. Anal., 48(1), 320—348, 2016.

[5] S. Amstutz and N. Van Goethem, *Incompatibility-governed elasto-plasticity for continua with dislocations*, Proc. R. Soc. A, 473(2199), 2017.

[6] B. Bakó, E. Clouet, L.M. Dupuy, and M. Blétry, *Dislocation dynamics simulations with climb: kinetics of dislocation loop coarsening controlled by bulk diffusion*, Phil. Mag., 91(23):3173–3191, 2011.

[7] W. Bao and J.G. Liu, *Dynamics in Models of Coarsening, Coagulation, Condensation and Quantization*, Lecture Notes Series, Institute for Mathematical Sciences, National University of Singapore. World Scientific, 9, 2007.

[8] V. Berdichevsky, *Continuum theory of dislocations revisited*, Cont. Mech. Therm., 18(9):195–222, 2006.

[9] J. Bolik and W. von Wahl, *Estimating ∇u in terms of div u, curl u, either (ν, u) or $\nu \times u$ and the topology*, Math. Meth. Appl. Sci., 20(9):737–744, 1997.

[10] R.W. Cahn, *Recrystallization of single crystals after plastic bending*, J. Inst. Metals, 76:121, 1949.

[11] E.A. Carlen, M.C. Carvalho, and E. Orlandi, *Approximate solutions of the Cahn–Hilliard equation via corrections to the Mullins–Sekerka motion*, Arch. Ration. Mech. Anal., 178(1):1–55, 2005.

[12] M.C. Delfour and J.P. Zolésio, *Shapes and Geometries: Metrics, Analysis, Differential Calculus, and Optimization, Second Edition*, Advances in Design and Control, Society for Industrial and Applied Mathematics (SIAM), Philadelphia, PA, 4, 2001.

[13] A.I. Bashtova, I.O. Lysenko, D.O. Kharchenko, and O.M. Schokotova, *A study of phase separation processes in presence of dislocations in binary systems subjected to irradiation*, Condensed Matter Physics, 18(2), 2015.

[14] R.D. Doherty, *Recrystallization and texture*, Progress in Material Science, 42(1-4):39–58, 1997.

[15] B.L. Eyre and D.M. Maher, *Neutron irradiation damage in molybdenum. part v. mechanisms of vacancy and interstitial loop growth during post-irradiation annealing*, Phil. Mag., 24(190):767–797, 1971.

[16] S.P. Fitzgerald and Z. Yao, *Shape of prismatic dislocation loops in anisotropic α-fe*, Phil. Mag., 9(89):581–588, 2009.

[17] F.A. Garner, N.H. Packan, and A.S. Kumar, *Radiation-induced Changes in Microstructure: 13th International Symposium (part I)*, ASTM Committee E-10 on Nuclear Technology, and Applications, ASTM, 289–314, 1987.

[18] J. Grabmaier, *Silicon*, Crystals, Springer Berlin Heidelberg, 2013.

[19] K. Gururaj, C. Robertson, and M. Fivel, *Channel formation and multiplication in irradiated fcc metals: a 3d dislocation dynamics investigation*, Phil. Mag., 95(12):1368–1389, 2015.

[20] P.B. Hirsch, J. Silcox, R.E. Smallman, and K.H. Westmacott, *Dislocation loops in quenched aluminium*, Phil. Mag., 3(32):897–908, 1958.
[21] T. Hochrainer, *Thermodynamically consistent continuum dislocation dynamics*, J. Mech. Phys. Solids, 88:12–22, 2016.
[22] T. Hochrainer and A. El-Azab, *A sharp interface model for void growth in irradiated materials*, Phil. Mag., 95(9):948–972, 2015.
[23] K. Jin, L.K. Béland, F. Zhang, T. Yang, L. Qiao, Y. Zhang, H. Bei, H.M. Christen, R.E. Stoller, and L. Wang, *Direct observation of defect range and evolution in ion-irradiated single crystalline ni and ni binary alloys*, Scientific Reports, 6:255507, 2016.
[24] E. Kröner, *Continuum theory of defects*, R. Balian, editor, Physics of Defects (Les Houches, Session XXXV, 1980), North-Holland, Amsterdam, 215–315, 1981.
[25] F. Kroupa, *Dislocation dipoles and dislocation loops*, Journal de Physique Colloques, C3(27):154–167, 1966.
[26] J.S. Langer, *Instabilities and pattern formation in crystal growth*, Rev. Mod. Phys., 52:1–28, Jan. 1980.
[27] N.Q. Le, *A Gamma-convergence approach to the Cahn–Hilliard equation*, Calc. Var. Part. Diff. Eqs., 32(4):499–522, 2008.
[28] G. Maggiani, R. Scala, and N. Van Goethem, *A compatible-incompatible decomposition of symmetric tensors in L^p with application to elasticity*, Math. Meth. Appl. Sci., 38(18):5217–5230, 2015.
[29] W.W. Mullins and R.F. Sekerka, *Morphological Stability of a Particle Growing by Diffusion or Heat Flow*, J. Appl. Phys., 34(4):323–329, 1963.
[30] F.R.N. Nabarro, *Strength of solids*, in Report of a Conference on Strength of Solids, University of Bristol, 1947, The Physical Society, London 1948.
[31] M. Niewczas, O. Engler, and J.D. Embury, *The recrystallization of Copper single crystals deformed at 4.2K*, Acta Materialia, 52(3):539–552, 2004.
[32] A. Novick-Cohen, *The Cahn–Hilliard equation*, in Handbook of differential equations: Evolutionary equations, Amsterdam: Elsevier/North-Holland, IV:201–228, 2008.
[33] F. Otto, C. Seis., and D. Slepčev, *Crossover of the coarsening rates in demixing of binary viscous liquids*, Commun. Math. Sci., 11(2):441–464, 2013.
[34] R.L. Pego, *Front migration in the nonlinear Cahn–Hilliard equation*, Proc. R. Soc. Lond., Ser. A, 422(1863):261–278, 1989.
[35] M.A. Peletier, *Energies, gradient ows, and large deviations: a modelling point of view*, Lecture notes, Pisa, 2011.
[36] J. Philibert, *Atom Movements: Diffusion and Mass Transport in Solids*, Monographies de Physique. Editions de Physique, 1995.
[37] J. Rahed, *Defects in Crystalline Silicon: Integrated Atomistic and Continuum Modeling*, PhD thesis, Israel Institute of Technology, Haifa, Israel, 2009.
[38] M.N. Shetty, *Dislocations and Mechanical Behaviour of Materials*, PHI Learning, 2013.
[39] P.A. Beck and P.P. Sinha, *Polygonization in Bent Zinc Crystals*, J. Appl. Phys., 32(7):1222–1226, 1961.
[40] T. Sinno, *Defects in Crystalline Silicon: Integrated Atomistic and Continuum Modeling*, PhD thesis, Massachusetts Institute of Technology, USA, 1998.
[41] R.J. Stokes and C.H. Li, *Dislocation configurations and the initiation of yielding in Magnesium Oxide*, Discuss. Faraday Soc., 38:233–242, 1964.
[42] T.D. Swinburne, K. Arakawa, H. Mori, H. Yasuda, M. Isshiki, K. Mimura, M. Uchikoshi, and S. L. Dudarev, *Fast, vacancy-free climb of prismatic dislocation loops in bcc metals*, Scientific Reports, 6:30596, 2016.
[43] L. Tartar, *On Homogenization and Γ-convergence*, Homogenization, 2001 (Naples), GAKUTO Internat. Ser. Math. Sci. Appl., Gakkōtosho, Tokyo, 18:191—211, 2003.
[44] R.J.D. Tilley, *Defects in Solids*, Special Topics in Inorganic Chemistry, Wiley, 2008.
[45] N. Van Goethem, *Cauchy elasticity with dislocations in the small strain assumption*, Appl. Math. Lett., 96:94–99, 2015.
[46] N. Van Goethem, *Direct expression of incompatibility in curvilinear systems*, The ANZIAM J., 58(1):33–50, 2016.
[47] N. Van Goethem, *Dislocation-induced linear-elastic strain dynamics by a Cahn-Hilliard-type equation*, Math. Mech. Compl. Syst., 4(2):169–194, 2016.
[48] N. Van Goethem, *Incompatibility-governed singularities in linear elasticity with dislocations*, Math. Mech. Solids, 22(8):1688–1695, 2017.
[49] N. Van Goethem and F. Dupret, *A distributional approach to 2D Volterra dislocations at the continuum scale*, Europ. J. Appl. Math., 23(3):417–439, 2012.
[50] C.R. Weinberger and G.J. Tucker, *Multiscale Materials Modeling for Nanomechanics*, Springer

Series in Materials Science, Springer International Publishing, 245, 2016.
[51] S.J. Zinkle, *Radiation-induced effects on microstructure*, Rudy J.M. Konings, editor, in Comprehensive Nuclear Materials, Elsevier, Oxford, 1:65–98, 2012.